Semi-Annual Technical Report

V6061 (Formerly T6142)

ANALYSIS OF IONOSPHERIC DATA

Prepared by

Robert D. Sears

of

IIT RESEARCH INSTITUTE
Chicago, Illinois 60616

"Research Sponsored by the Advanced Research Projects Agency (ARPA Order No. 749) through the Office of Naval Research, Contract No. N00014-66-C0030 Task No. NR 088-029"

June 1968

65

Semi-Annual Technical Report

V6061 (Formerly T6142)

ANALYSIS OF IONOSPHERIC DATA

ARPA Order No. 749

Contract No. N00014-66-C0030

1 October,1967 to 31 March, 1968

Distribution of this document is unlimited

Prepared by

Robert D. Sears

of

IIT RESEARCH INSTITUTE
Chicago, Illinois 60616

"Research Sponsored by the Advanced Research ProjectsAgency (ARPA Order Nc. 749) through the Office of Naval Research, Contract No. N00014-66-C0030, Task No. NR 088-029"

June 1968

FOREWORD

This is the fourth semi-annual technical report covering research performed under the Office of Naval Research Contract No. N00014-66-C0030, ARPA Order No. 749, entitled, "Analysis of Ionospheric Data". This report covers research performed during the contract period 1 October 1967 to 31 March, 1968. The contract is under the technical cognizance of Mr. R. Gracen Joiner of ONR and Lt. Col. J. K. LeRohl of ARPA.

The research reported herein covers the second phase effort under the subject contract, the determination of short term fluctuations in electron density in the lower ionosphere as measured by simultaneous doppler dispersion and amplitude effects on HF signals. The power spectra of the apparent doppler frequency on three HF frequencies are compared during quiet dawn periods (some of which were reported in the last report), geomagnetically disturbed dawn periods, and during quiet and disturbed daytime periods. Interpretation of the doppler dispersion characteristics of the HF signals as well as the average doppler signatures in terms of the level detection of the ionospheric changes caused by nuclear bursts and discrimination of these effects from natural signals is presented.

Contributing to the research during this period were Dr. G. L. N. Rao, Mr. G. Owen, and R. D. Sears.

Respectfully submitted,

IIT RESEARCH INSTITUTE

Robert D. Sears
Senior Scientist,
Group Leader
Plasma Physics

APPROVED BY:

William O. Davies
Assistant Director
Physics Division

ABSTRACT

The average and short term fluctuations in apparent doppler frequency imposed upon three high frequency short-hop propagation paths are described. The average variation in doppler frequency during development of the reflecting region at dawn for both geomagnetically disturbed and quiet conditions can be characterized by an exponentially decaying positive doppler signal. The small scale doppler frequency fluctuations are analysed by power spectral analysis techniques. It is shown that the power spectra usually have a constant spectral intensity at higher frequencies (e.g. a white spectrum), and a slightly increasing spectral intensity at lower frequencies (e.g. a pink spectrum). The power contained in the white portion of the spectrum is shown to be correlated with the geomagnetic activity index ΣK_p.

The average changes in doppler frequency for quiet and disturbed dawns and for quiet and disturbed daytime periods are related to the determination of the level of range and x-ray yield at which nuclear bursts in space may be detected against the natural background. Also, the natural fluctuation level of the hf doppler signals is related to the level of x-ray yield and range at which nuclear burst effects can be distinguished from the natural doppler "noise" level of an hf detection system.

TABLE OF CONTENTS

I. SUMMARY

The purpose of the research reported herein is to determine the long and short term changes in electron density in the lower ionosphere under different conditions of geomagnetic disturbance. Short term changes of the electron content in the lower ionosphere and in the hf signal reflection altitude limit the detection level of the ionospheric effects of nuclear bursts in space: the lower limit of burst yield which can be detected is determined by the ionospheric electron density background fluctuation level. Better specification of the electron density changes and their effects upon hf propagation allows better discrimination between natural ionospheric changes and the ionospheric effects of high altitude nuclear bursts.

This study of the natural ionospheric phase and amplitude fluctuations on an hf signal was designed to include a variety of data. The data base includes high frequency phase and amplitude data on a three frequency, single hop propagation path between Tutuila (American Samoa) and Tongatapu which were obtained during the summer and fall of 1962. Supporting data in the form of ionograms and true height analyses (furnished by J. W. Wright of ITSA) are also utilized.

The apparent doppler frequency and the amplitude of the signal are utilized to determine the parameters which affect

nuclear burst detection and discrimination. The level of detection of a nuclear burst depends upon the natural ionospheric background doppler frequency and amplitude changes on the received hf signal. In this investigation we have concentrated upon the characterization of the average doppler frequency during periods of propagation path change (on controlled single hop paths) in order to determine the effects which the gain or loss of a reflection point have upon average doppler frequency. For several dawns, including periods of both geomagnetic quiet and disturbance, the characteristic signature of the doppler frequency on the signals is established in order to separate it from the small scale variations. When the average behavior of the apparent doppler frequency can be established, the small scale variations determine the detection level for nuclear burst effects. In order to determine whether any preferential time scales exist for the small scale doppler signal variations, power spectra of the variations for both dawn intervals and for selected daytime periods were computed. Determination of the average doppler power in given spectral regions then aids in discriminating natural ionospheric signals from those induced by nuclear bursts.

During the research period reported herein, the characterization of average doppler signatures for the geomagnetically disturbed dawn periods has continued. The method of analysis was similar to that used for the quiet dawn periods. Several doppler frequency pattern features were found in the disturbed dawn which were not found in the quiet dawns. Because the propagation path in the pre-dawn period is generally caused by scatter from F region inhomogenieties, the pre-dawn doppler frequencies can be related to movement, or rate of change of density in the scattering inhomogenieties. During the disturbed pre-dawn periods, the doppler frequency is significantly higher than for quiet periods. This observation is consistent with the expected behavior of the upper F region during disturbed geomagnetic conditions. Prior to the development of a specularly reflecting layer, the doppler frequency is greatly reduced. This reduction is more pronounced during disturbed periods because of the relatively high values of pre-dawn doppler frequency. As the layer forms and reflecting conditions are established, the large positive doppler excursion and its subsequent exponential decay in time closely follow the quiet dawn behavior.

The residue of the doppler signal is calculated by subtraction of the average doppler frequency trend at dawn from the measured values. The resulting doppler signal fluctuations have a near zero average value. Power spectra of the fluctuating doppler signal indicate an overall higher fluctuation power for geomagnetically disturbed days than for quiet days. In addition, several instances of apparently significant power in quasi-periodic disturbances were found.

Power spectral analysis of hf doppler frequency fluctuations was extended to the daytime data for both quiet and disturbed days. The time period chosen for this extension of the analysis was 2100 to 0100 GMT or 1000 to 1400 Local time. Again, disturbed days showed appreciably larger values of average doppler frequency dispersion.

Interpretation of doppler dispersion and doppler power spectra in terms of nuclear burst detection and discrimination results can be simply summarized. The apparent doppler frequency shift on the hf signal is directly related to the rate of change of electron content along the signal path if the reflection point remains constant. Hence, impulsive ionization from a nuclear burst results in an initially very high positive doppler excursion which may be unmeasurable, followed by a slowly decaying negative doppler signal. If the ionization is in the lower ionosphere and is relatively weak, the ionization and the doppler signal both decay approximately exponentially (at nighttime). If the ionization is relatively intense (for both nighttime and daytime) a saturation phenomena occurs, after which the decay is either linear or quadratic. If the characteristic time associated with the decay of the nuclear burst ionization lies in a region in which there are appreciable natural variations, then the discrimination of the burst effect from naturally occurring effects will be degraded for a given burst yield, even though the doppler signal may be great enough to detect. Hence, examination of the natural doppler fluctuation spectra yields a useful measure of the discrimination level.

Likewise, the dependence of the doppler frequency on the received signal strength and the natural variations imposed by ionospheric phenomena influence the detection level of nuclear burst effects. In many cases ionospheric changes produce average doppler variations in signal frequency as great as 1 to 10 Hz during development of a layer at dawn. If average behavior under these natural conditions can be successfully characterized or modeled, then the detection threshold may be reduced to the level of the doppler fluctuations away from average, that is, the 0.03 to 0.1 Hz range.

II. TECHNICAL DISCUSSION

A. Average Doppler Frequency at Dawn and Daytime

The average doppler frequency on the three frequencies utilized in the experiment was determined for ten dawn and for five daytime intervals. The dates, times, and geomagnetic disturbance conditions covered by the data are summarized in Table I. The average doppler signal behavior during the dawn and daytime intervals may be characterized by a typical signature, the parameters of which may then be examined for their dependence upon geomagnetic or other disturbance indices.

The dawn period data for quiet geomagnetic conditions were summarized in the last report[1] on this contract and the signature definition procedure was explained. It was found that after establishment of "specular" reflection conditions from the ionospheric F region after dawn, the average doppler frequency had a characteristic exponential decay from a positive value of about 1 Hz. This pattern occurred at all observed frequencies and on ordinary and extraordinary magnetoionic wave signals when both could be observed. This characteristic signature is illustrated in Figure 1 and it may be described by two parameters: the initial doppler frequency and the exponential decay time constant.

Parametric description of dawn period data for disturbed days was accomplished during the last semi-annual reporting

TABLE I DOPPLER FREQUENCY DATA - DAWNS

DATE	TIME GMT	FREQUENCY (MHz)	MODE	GEOMAGNETIC K_p INDEX Day	GHr	INITIAL DOPPLER FREQUENCY VALUE (Hz)	EXPONENTIAL SLOPE (sec^{-1})
10/15	1731-1751	9	$1F_o$	18q	4	0.83	-0.0522
	1751-1941	9	$1F_o$	18q	4	0.206	-0.00156
10/17	1716-1808	4	$1F_o$	13	1	1.04	-0.0251
	1701-1721	6	$1F_o$	13	1	1.27	-0.0533
	1721-1840	6	$1F_o$	13	1	0.361	-0.0132
	1751-1859	9	$1F_o$	13	1	0.273	-0.00812
10/18	1707-1750	4	$1F_o$	22	6	0.720	-0.0305
	1646-1753	6	$1F_o$	22	6	0.69	-0.0288
	1720-1752	9	$1F_{x/o}$	22	6	1.09	-0.542
	1752-1902	9	$1F_o$	22	6	0.231	-0.010
10/19	1720-1815	9	$1F_o$	27	9	0.513	-0.139
10/20	1709-1811	4	$1F_o$	19q	6	0.988	-0.0192
	1730-1823	6	$1F_o$	19q	6	0.309	-0.0168
	1738-1903	9	$1F_o$	19q	6	0.257	-0.00684
10/22	1645-1830	6	1F	29	6	1.15	-0.0194
	1643-1830	9	1F	29	6	1.63	-0.0251
10/23	1701-1830	4	1F	29	7	0.807	-0.117
	1659-1835	6	1F	29	7	0.545	-0.00878
	1657-1954	9	1F	29	7	0.576	-0.011
10/25	1610-1840	4	1F	35D	10	1.15	-0.104
10/26	1640-1803	6	1F	34D	9	0.815	-0.0203
	1636-1811	9	1F	34D	9	1.68	-0.324
	1811-1938	9	1F	34D	9	0.18	-0.00932
10/27	1648-1754	6	1F	31	8	0.611	-0.0193
	1650-1815	9	1F	31	8	0.750	-0.022

Local Time = GMT - 11 Hours

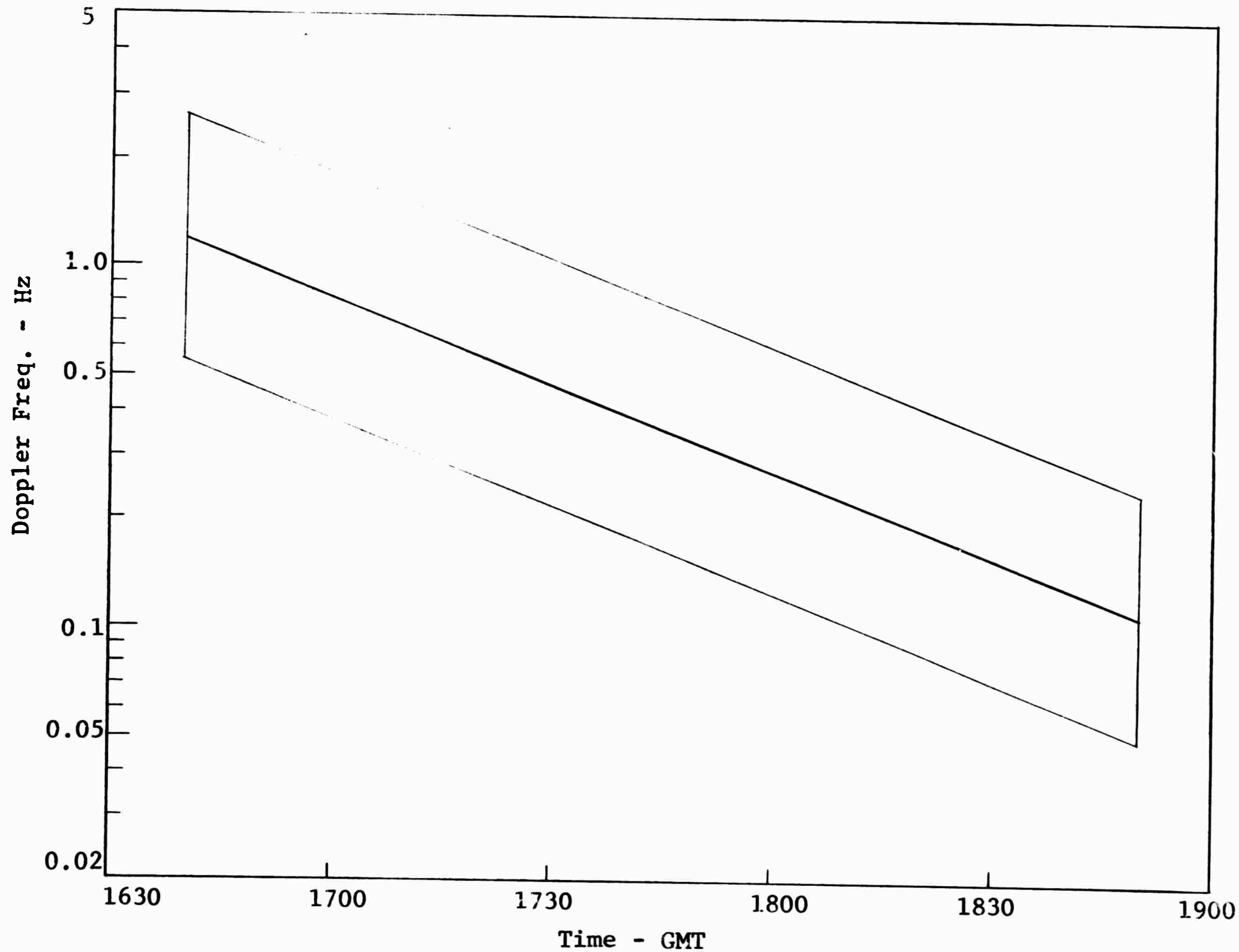

Figure 1 Average Doppler Frequency Signature for Dawn Doppler Data (10 days)

period and confirmed the validity of the approach. Typical doppler frequency behavior during a quiet dawn and during a geomagnetically disturbed dawn is illustrated in Figures 2 and 3. Comparison of the initial doppler frequencies and the time constant (obtained from the exponential slopes of the frequency vs. time curves) for different frequencies and different disturbance indices does not indicate significant dependence of the parameters on either transmitted frequency or geomagnetic disturbance. The outlined area in Figure 1 contains essentially all of the observed doppler frequency traces with the possible exception of flare effects which occurred on the 15th, 18th, and 23rd.

The pre-dawn doppler frequency behavior appears to be highly erratic and dependent upon the degree of geomagnetic disturbance. In general, when a coherent doppler frequency can be determined quantitatively, the average doppler is higher during high geomagnetic disturbance dawns. A correlation plot of pre-dawn doppler frequency value versus disturbance index did not yield an observable correlation, however. This is probably due to the intermittent qualitity of the data and the difficulty of interpretation for high magnetic disturbance nights. Figures 2 and 3 qualitatively illustrate the pre-dawn scattering doppler frequency effects for quiet and disturbed periods.

The propagation path in the pre-dawn period is created by scattering of the signal from irregularities in the F region

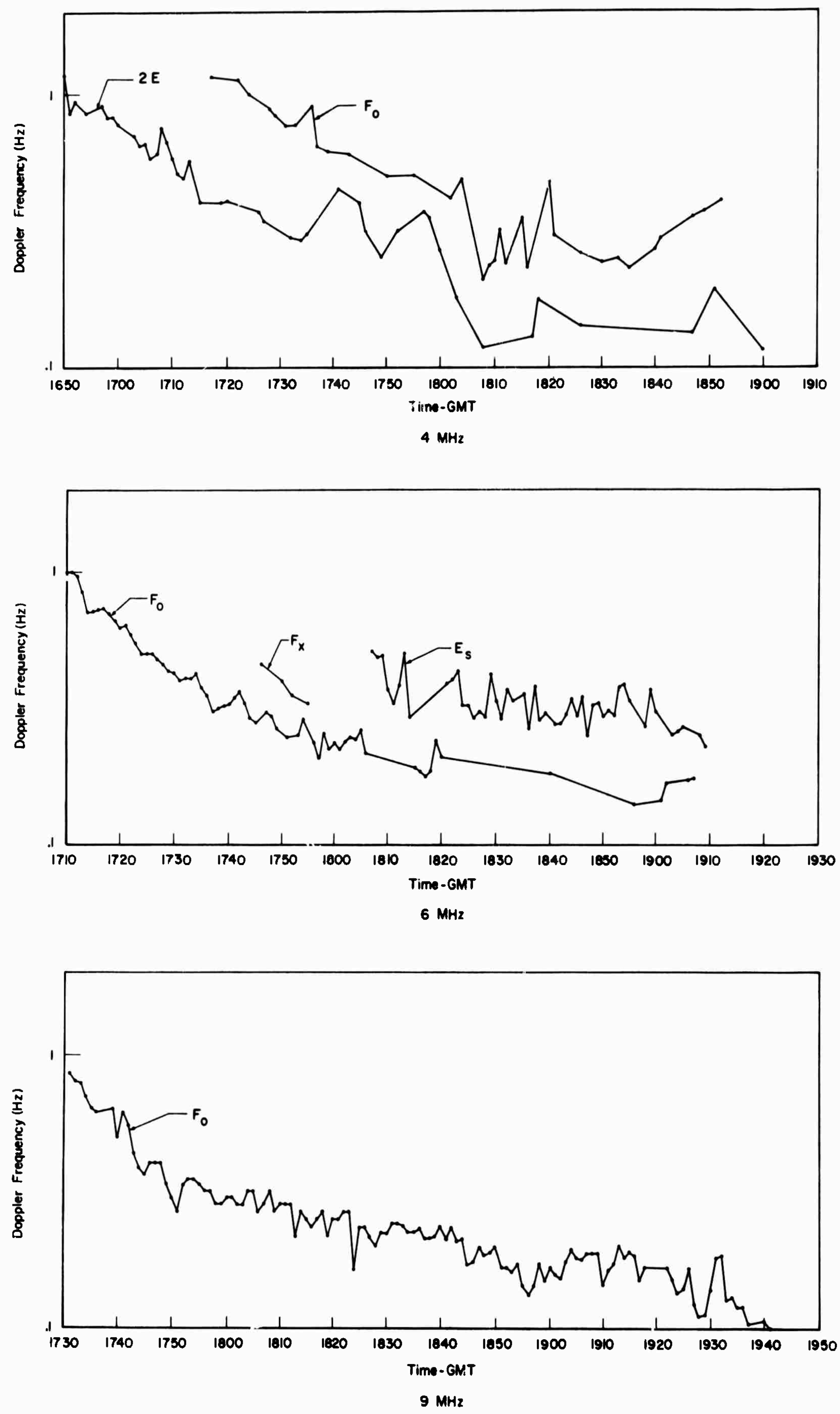

Figure 2 Doppler frequency vs. time for a geomagnetically quiet dawn period.

1630-1940 GMT, 0530-0840 LT 10/15/62

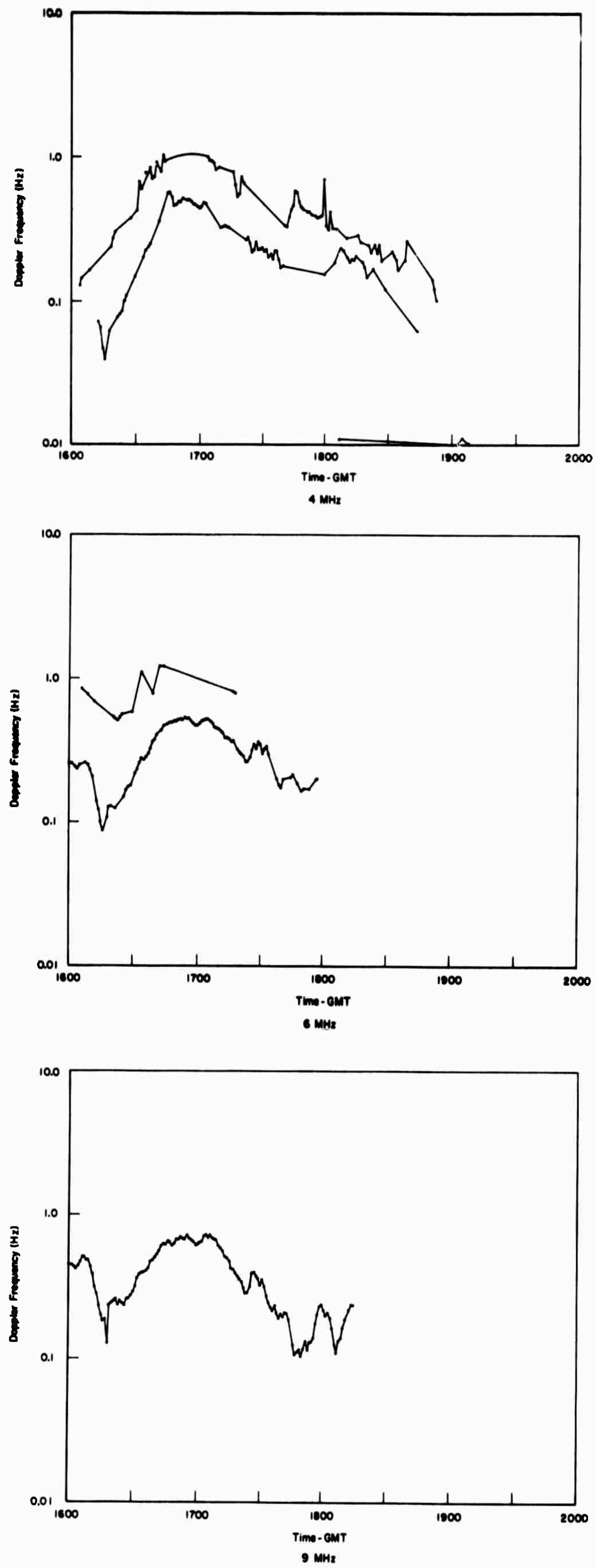

Figure 3 Doppler frequency vs. time for a geomagnetically disturbed dawn period.

1600-1900 GMT, 0500-0800 LT 10/27/62

rather than "specular reflection" from the F layer. In disturbed conditions, inhomogeniety changes and ionospheric motions tend to be greater, hence these would induce a higher average and a more highly variable doppler frequency on the scattered signals. Thus, although quantitative information cannot be obtained from this portion of the data, the qualitative observations seem to agree with the physical processes known to occur.

Daytime doppler frequencies are characteristically of very low value (i.e., in the 0.01 to 0.1 Hz range) for all frequencies and for a large range of magnetic disturbance indices. Figures 4 and 5 illustrate daytime data for a quiet period and for a geomagnetically disturbed period. (2200-2300 GMT on 15 October and 17 October, 1962). Comparisons of average doppler frequency in the daytime for geomagnetically disturbed and quiet conditions, show no obvious correlation with geomagnetic disturbance for any of the observed frequencies. On the other hand, the variability of the data from the average (i.e. random and periodic fluctuations in the received doppler frequency due to changes in electron density and reflection level in the ionosphere) is significantly affected by geomagnetic disturbances. A hint of this is shown in Figure 4 and 5 and the details of the analysis of this effect by power spectral analysis is contained in a following section.

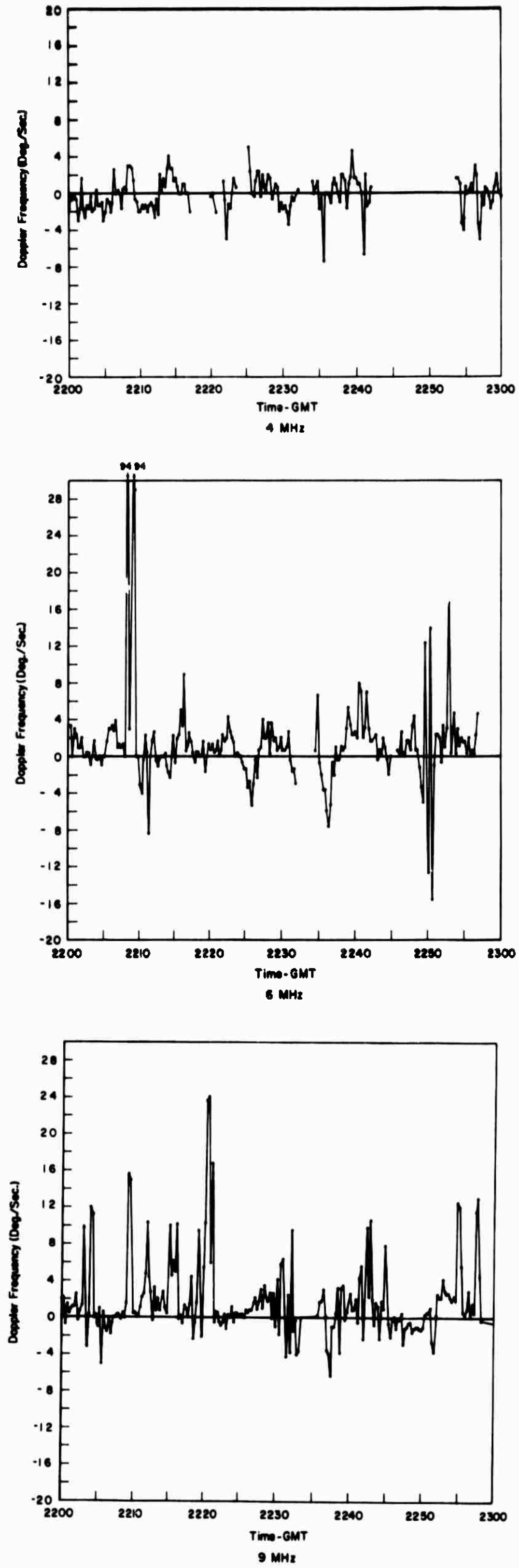

Figure 4 Doppler frequency vs. time for a geomagnetically quiet daytime period.

2200-2300 GMT, 1100-1200 LT 10/15/62

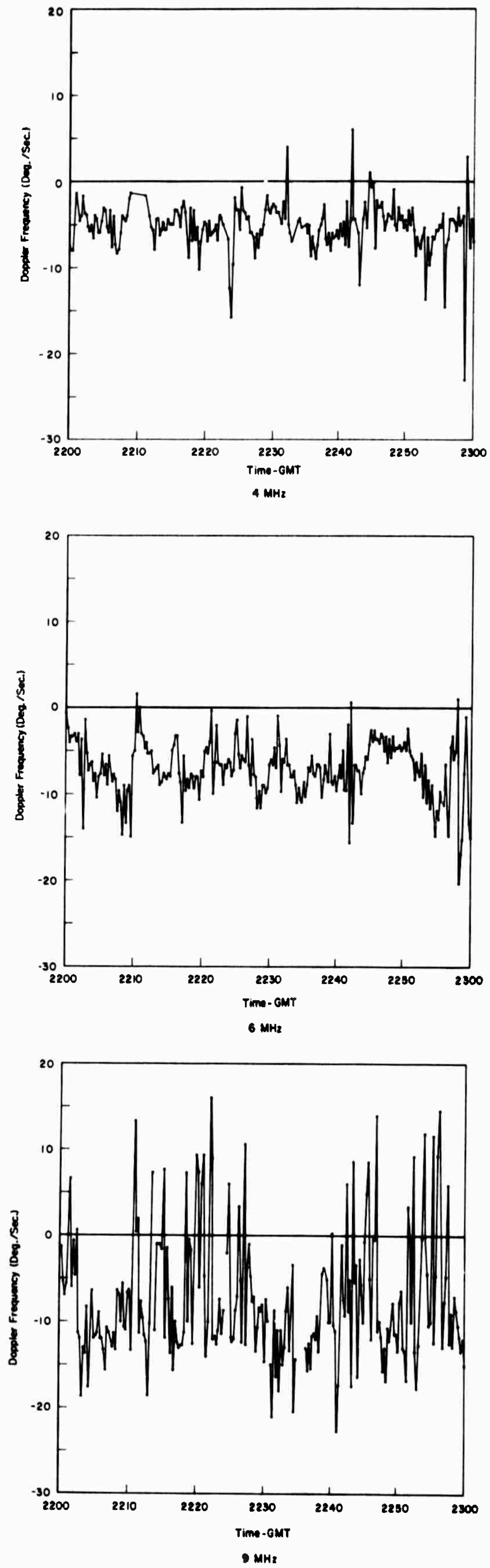

Figure 5 Doppler frequency vs. time for a geomagnetically disturbed daytime period.

2200-2300 GMT, 1100-1200 LT 10/27/62

B. Doppler Power Spectra

The power spectra of the variations of doppler frequency about average behavior have been computed for five disturbed dawns, five quiet dawns (reported in semi-annual report number 3), and for five daytime intervals covering both quiet and disturbed conditions. The spectra were computed for each transmitted frequency for identical time intervals whenever possible. The specific dates, times and frequencies for which power spectra have been computed are listed in Table II. In most cases, omission of a particular data interval was the result of an insufficient number of doppler frequency points being available in a consecutive time period, or the time period of good data being too short to allow a meaningful spectrum computation. The computational technique requires data at constant time intervals; hence, missing data points must be filled by interpolation. The data reduction interval was 1 minute for dawn data and 15 seconds for daytime records. Thus the spectrum extends from the lower frequency, which is determined by the record length, to the upper or nyquist frequency, which is determined by the data interval (0.033 Hz in the daytime cases and 0.0086 Hz for dawns). In both cases, estimated fluctuation power introduced by the sampling procedure is considerably less than that found in the data. The doppler frequency power spectral results presented in the last report were also rerun with an improved average doppler subtraction

TABLE II DOPPLER FREQUENCY POWER SPECTRAL COMPUTATIONS

DATE	TIME INTERVAL	FREQUENCY	SPECTRAL SHAPE
10/15	1751-1941GMT	9 MHz	Pink
10/15	2100-0100	4 MHz	Pink
	2100-0100	6 MHz	Enhanced
	2100-0100	9 MHz	Pink
10/17	1721-1840	6 MHz	Pink
	1715-1859	9 MHz	Pink
10/18	1656-1753	6 MHz	Pink
	1650-1752	9 MHz	Enhanced
	1752-1902	9 MHz	Enhanced
10/19	1720-1815	9 MHz	Pink
10/20	1730-1823	6 MHz	Red
	1738-1903	9 MHz	Red
10/22	1643-1830	9 MHz	Pink
10/23	1701-1830	4 MHz	Enhanced
	1659-1835	6 MHz	Pink
10/25	1610-1840	4 MHz	Pink
10/26	1640-1803	6 MHz	Red
10/27	1648-1754	6 MHz	Pink
	1650-1815	9 MHz	Pink
	2100-0100	4 MHz	Pink
	2100-0100	6 MHz	White
	2100-0100	9 MHz	White

routine and a better spectral estimate smoothing procedure.

Power spectra on three frequencies during quiet and disturbed dawns are presented in Figures 6 and 7. Although the degree of smoothing of these spectra is still not entirely satisfactory, the general trend of the spectral power vs. frequency can be observed. These spectra are typical of those which were denoted as "pink" spectra in the previous technical report; that is, the high frequency spectral density is nearly constant whereas a gradual rise in power is exhibited at low frequencies. Daytime power spectra, Figures 8 and 9, tend to be even smoother than those for the dawns. The overall spectral intensity is somewhat higher however for equivalent frequencies and disturbance levels.

The purpose of computing and displaying doppler power spectra of this type is to determine the degree of randomness of the doppler dispersion which would be denoted by a relatively "white" or constant spectral density curve. If the doppler frequency signals have small periodic disturbance components in them, the spectral estimate will have peaks at frequencies in the spectral range inversely proportional to the period of the disturbance. This type of disturbance could be produced by wavelike travelling disturbances in the ionosphere and is evident in the data at several instances. For example, apparently significant power increases or disturbances having periods of 3 and 6 minutes exist in the 9 MHz record of October 15th and a 5 minute periodicity exists in the 4 MHz record

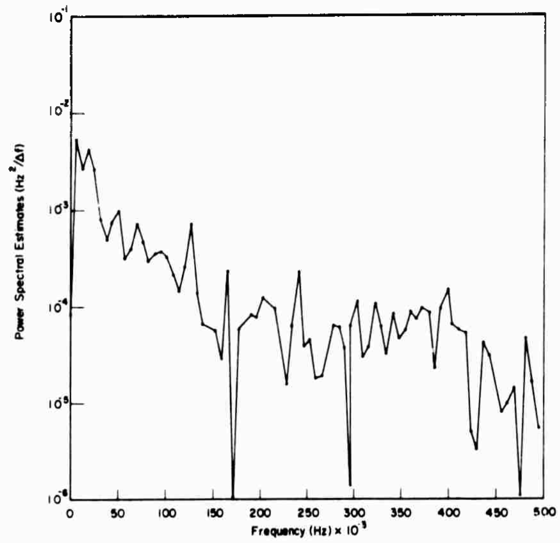

6 MHz F_0 1721-1840 GMT, 0621-0740 LT 10/17/62 $K_p = 0_0$

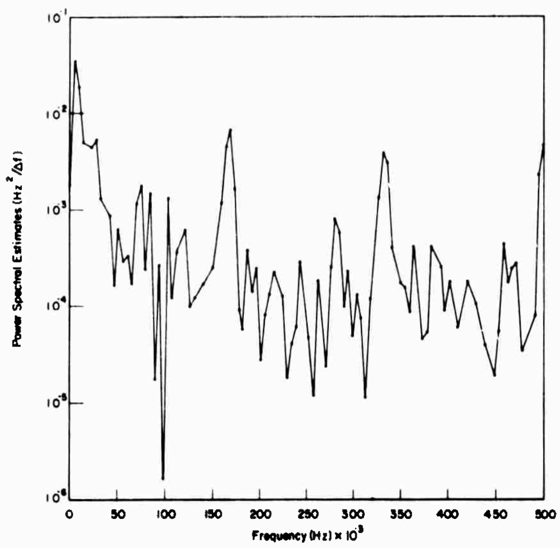

9 MHz F_0 1751-1941 GMT, 0651-0841 LT 10/15/62 $K_p = 3-$

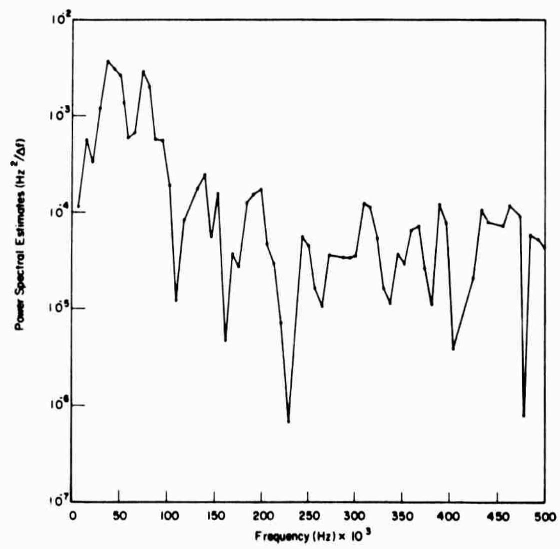

9 MHz F_0 1715-1859 GMT, 0615-0759 LT 10/17/62 $K_p = 0_0$

Figure 6 Power spectra of doppler frequency fluctuations for geomagnetically quiet dawn periods.

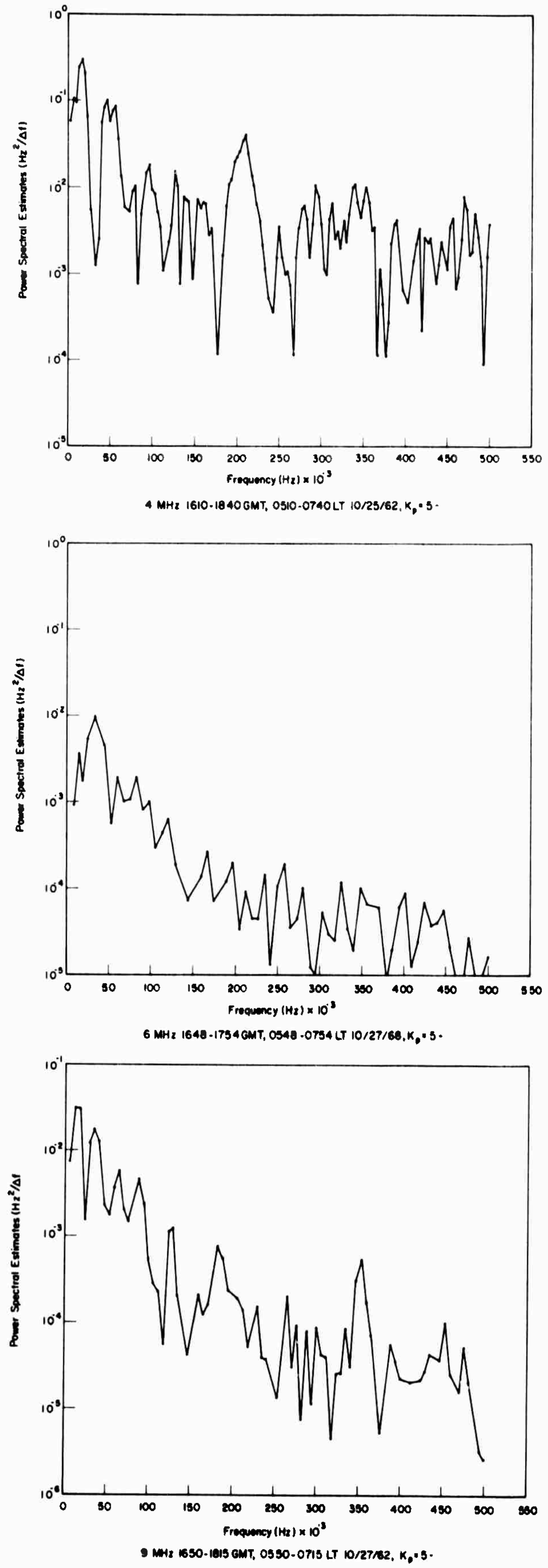

Figure 7 Power spectra of doppler frequency fluctuations during geomagnetically disturbed dawn periods.

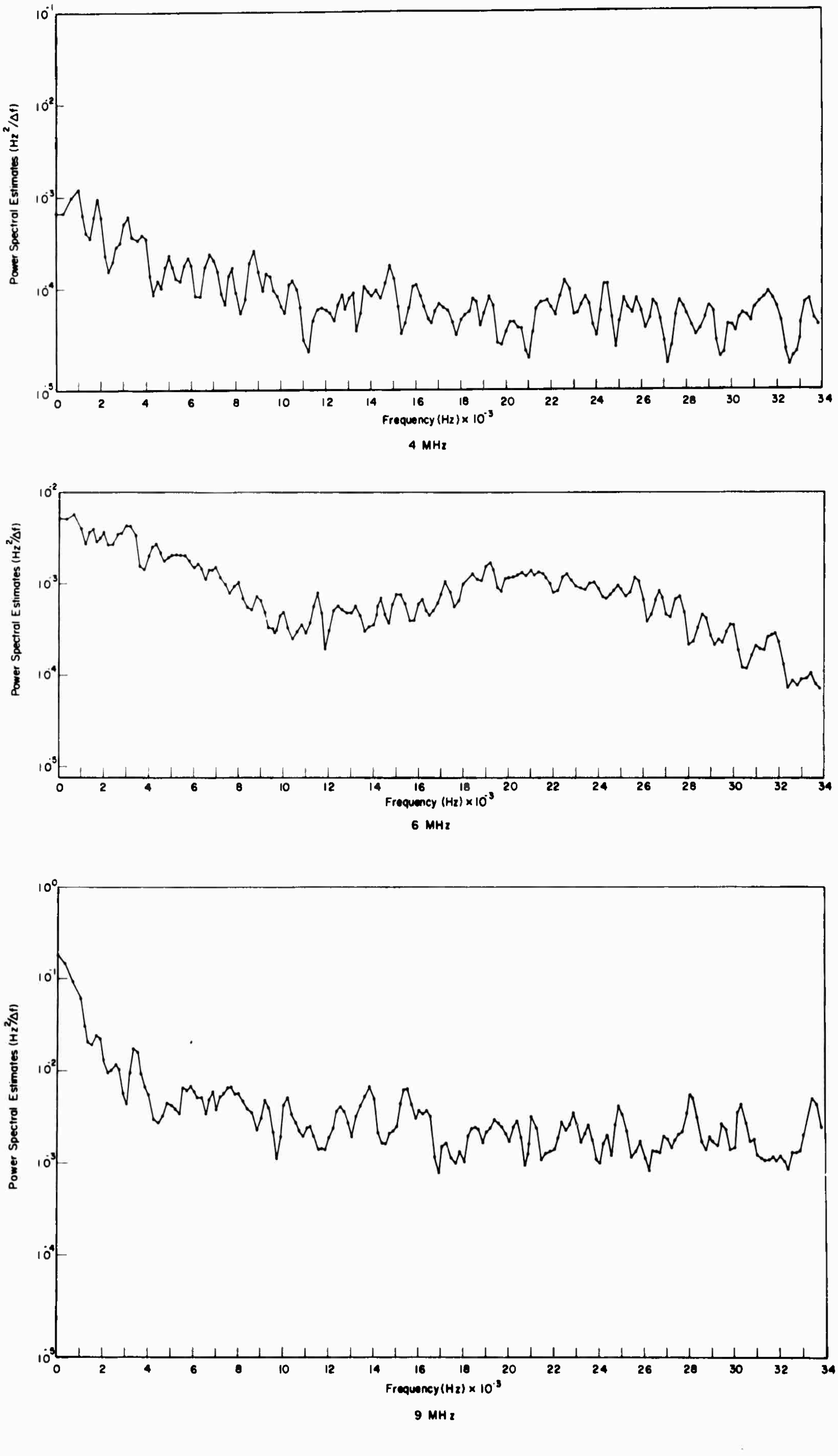

Figure 8 Power spectra of doppler frequency fluctuations during geomagnetically quiet daytime period.

2100-0100 GMT, 1000-1400 LT 10/15/62

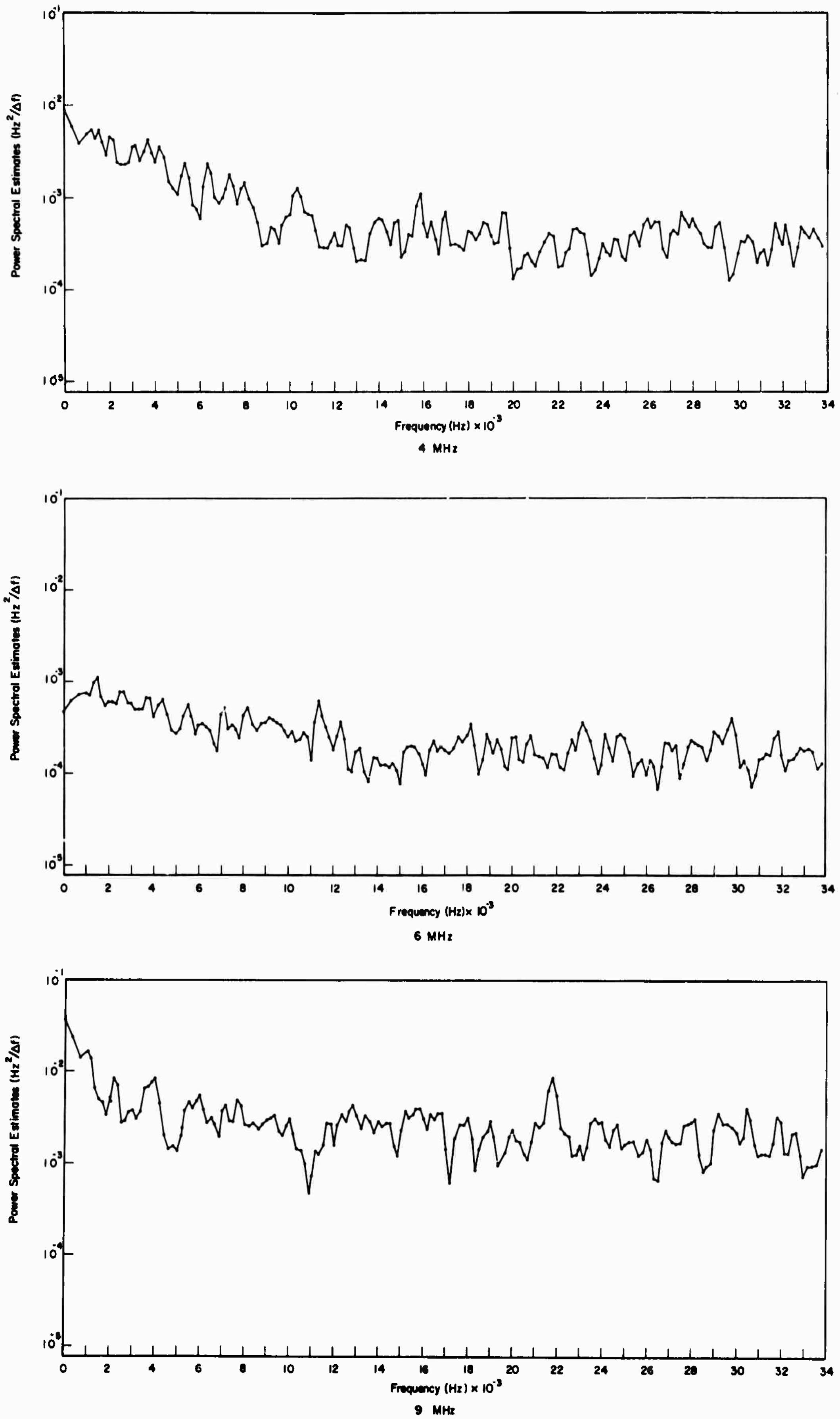

Figure 9 Power spectra of doppler frequency fluctuations during geomagnetically disturbed daytime period.

2100-0100 GMT, 1000-1400 LT 10/27/62 K_p = 3+

for October 25th. If travelling disturbances or other irregularities which cause doppler dispersion on the hf signal are nearly regular (that is, having a characteristic period which is distributed about a peak value), then their power spectrum will show this effect by having a corresponding wide peak. It is of interest to note that most of the dawn data do not show a significant number of peaks in spectral power except perhaps at relatively low frequency or long period.

The observed absence of strong coherent or broad band periodic distrubances in the data may be explained by one or more of the following: The data record analyzed is too long compared with the duration of the periodic disturbances to adequately separate their power from the normal randomness of the ionosphere; there are few or no periodic disturbances present in either the F region or the lower ionosphere during the intervals covered by the data; the experiment is not sensitive enough to pick up the disturbances. These hypotheses are examined in detail.

Sensitivity of the instrument in relating phase change or doppler frequency to changes in integrated electron density along the propagation path, or to the change in reflection height on the path, is easily determined. A measured doppler frequency of 0.01 Hz at 6 Mhz is equivalent to a rate of change in reflection height in the F region of about 0.7 meters per second. This degree of motion could be attained in the ionosphere with almost any change of electron density gradient caused by a disturbing mechanism. If the same apparent doppler frequency, 0.01 Hz, is related to the rate of change of ionization along the propagation path, an equivalent columnar density change of about 2×10^7 electrons/cm^2-sec is obtained. This value corresponds to a density fluctuation of 10^2 electrons/cm^3-sec in a 1 kilometer thin sporadic E layer or of 1 electron/cm^3-sec over the 100 km-200 km region at dawn. Hence, it may be concluded that small natural fluctuations of the order of 1 percent of the density of the dawn E region may be detected by the present system.

Characteristics of the spectral power computations tend to eliminate periods of highly variable doppler simply because of the requirement that doppler data must be obtained on a constant time interval basis. During highly disturbed periods, this data is not obtained consistently due to switching of the maximum signal between several propagation paths (e.g., high and low ray paths). Hence the periods of interest, containing high level periodic disturbances, in fact may be eliminated by this data reduction limitation.

The other hypothesis is that the short time duration of the periodic disturbance compared with the overall power spectral computation interval also limits the maximum power which could be detected from a periodic disturbance. In effect, the actual power in a short periodic disturbance is reduced by the computational procedure by a factor approximately proportional to the length of the disturbance divided by the length of the computational interval. Hence, if a periodic disturbance with a total duration of one tenth of the computational interval were present, and if its power were about 10 times the random power present in the remaining disturbances in this frequency interval, then the observed peak would be only a factor of 2 larger than the other random components. A factor of 2 is about the minimum detectible spectral power peak in the current data.

It must be concluded that observation of so few statistically significant periodic disturbances in the doppler data and hence in the ionospheric electron density changes is caused by a combination of lack of large natural events in the data interval analyzed, and by the relative insensitivity of the computational procedure (not the instrumentation) to short duration periodic disturbances. As is shown in the next section, however, the computational procedure limitation for periodic events does not place a serious limit on interpretation of the background random doppler data in terms of limits on nuclear burst ionization detection and discrimination.

The "white" portion of the noise power spectrum for doppler frequency was examined in detail with respect to its variation with transmitted frequency and with geomagnetic disturbances index. No significant variation with frequency was discovered; however, a geomagnetic disturbance does have an observable influence on overall doppler fluctuation power level. The correlation plot of average power in the flat portion (high frequency) of the doppler spectrum versus the geomagnetic disturbance index K_p (where the sum is over the two-three hour periods which include the data) is illustrated in Figure 10. A small group of points in the high disturbance but low fluctuation power portion of the graph indicates that fluctuation power does not always increase with geomagnetic disturbance. Also it appears that the lower frequencies which are reflected lower in the ionosphere may possess slightly less total fluctuation power than the 9 MHz points at the same times and at the same disturbance levels.

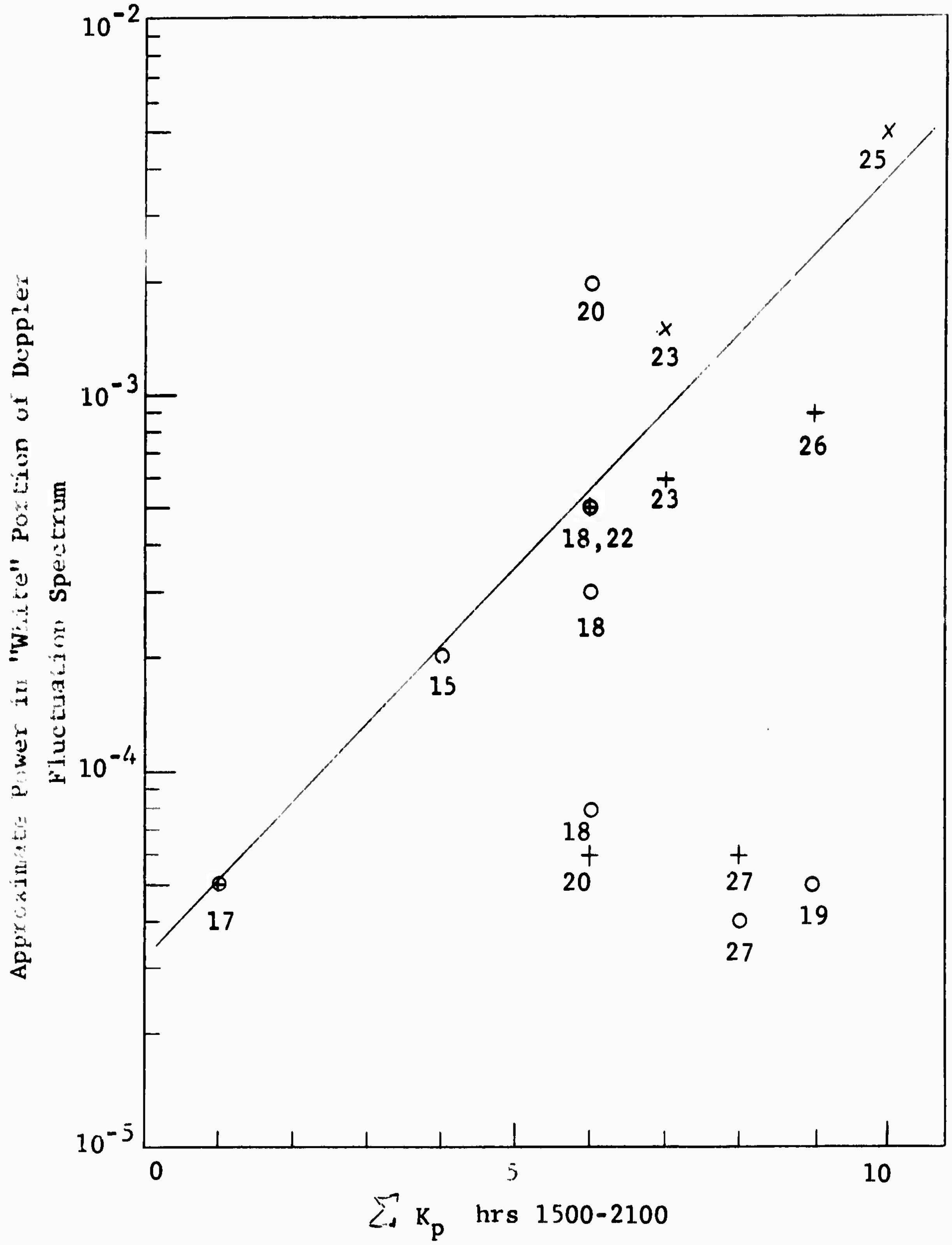

Figure 10 Variation of Average Power in White Portion of Doppler Spectrum vs. Magnetic Disturbance Index

III. DETECTION AND DISCRIMINATION THRESHOLDS FOR NUCLEAR BURSTS IN SPACE

A. General Background, Profile of X-Ray Ionization

Nuclear bursts in space radiate most of their energy as thermal x-rays with radiation temperature typically about 1 kev. The altitude profile of the ionization created by the transient x-ray flux incident upon the earth's atmosphere is sensitive to the radiation temperature of the burst as well as the zenith angle, x-ray yield, and distance from the earth. For bursts having temperatures between about 1/2 and 2 kev, the altitude profile is nearly constant except for the displacement of the ionization peak from the ground. In all cases, the ionization peak and hence the region of maximum effect lies in the D region. Figure 11 illustrates the variation in altitude of the ionization produced by the transient x-ray pulse before recombination begins.

Nuclear burst effects upon high frequency signals can be examined from two standpoints: (1) the peak excursion in hf phase and amplitude which is caused by the transient ionization can be compared with the magnitude of natural ionospheric events; (2) the time behavior of the decay of the ionization and its consequent time-varying effect upon the hf signal parameters can be examined and compared with natural values.

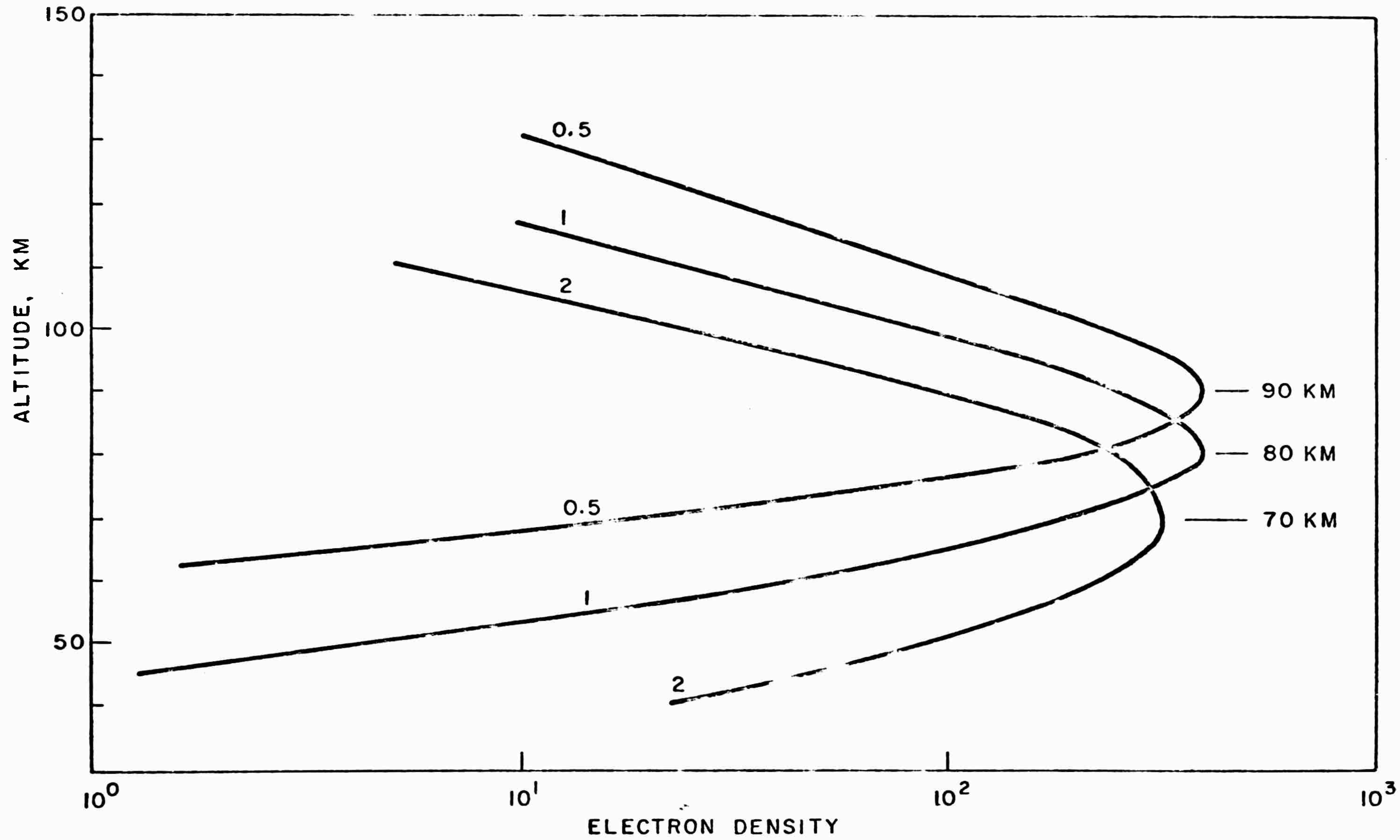

FIG. 11 TRANSIENT ELECTRON DENSITY VS. HEIGHT FOR X-RAY IONIZATION.

The nuclear bursts will be assumed to take place at local zenith at either local daytime or nighttime. The maximum phase path excursion caused by nuclear burst ionization and the apparent doppler frequency induced on the signal by the decay of the ionization will be compared to daytime and nighttime levels caused by natural disturbances. In g-neral, the maximum value of the phase excursion or maximum doppler frequency of the transient layer tends to define the detectability of the burst whereas the time variations compared with the natural fluctuations aid in discriminating small nuclear bursts from natural events in the ionosphere.

The altitude profile of x-ray ionization in the earth's lower ionosphere, which is illustrated in Figure 11 for several burst x-ray radiation temperatures, extends over several atmospheric density scale heights. Hence, computations of radio wave absorption and phase path change effects must take into account the altitude variation of the natural atmospheric parameters such as electron-neutral collision frequency. The ionized layer may be described in terms of a two parameter profile, the parameters are the peak electron content and the layer altitude z_c. The peak electron content is equal to be product of the peak electron density Ne (z_o) and the equivalent layer thickness T. The shape of the profile does not change appreciably over the range of x-ray temperatures (for zenith burst orientation) or over the range of deposition altitudes. The two parameter description of the ionization layer is called the "thin layer" approximation in the subsequent discussion and will be utilized to derive an altitude-independent formulation of phase path excursion doppler frequency and absorption conditions on hf signal paths passing through the ionized region.

In the thin layer approximation the altitude dependent electron density is given by

$$N_e\ (z) = N_e\ (z_o)\ T\ \delta\ (z - zo) \qquad (1)$$

where $N_e\ (z_o)$ is the peak electron density, T is the equivalent layer thickness; z_o is the altitude of the equivalent thin layer; $\delta\ (z - zo)$ is a Derac delta function of altitude z. If the peak density of the equivalent thin layer is set at that of the actual ionized layer, then the thickness of the equivalent thin layer is T = 11 km. Because of the rapid increase in electron - neutral collision frequency at lower altitudes, the altitude of the peak absorption in the actual ionized layer will be lower than the altitude of the equivalent thin layer. This correction is given as z (maximum absorption) = z_o -7 km. These values are derived from numerical integration of the x-ray ionization profile over the Appleton-Hartree form of the radio wave propagation integral.

B. Temporal Characteristics of Transient Ionized Layer Decay

A relatively straightforward series solution for the decay of ionization following a transient impulse has been developed.[2] The electron density as a function of time is given as

$$N_e(z,t) = \frac{A}{A+D}\,\frac{N_e(z,o)\,e^{-(A+D)\,t}}{(1+\alpha N_e(z,o)\,t)^{(\alpha_i/\alpha)}} + \frac{D}{D+A}\,\frac{N_e(z,o)}{1+\alpha N_e(z,o)\,t} \qquad (2)$$

where the altitude dependent and local time dependent parameters are

A - the attachment rate of electrons to neutral constituents

D - the detachment rate of electrons from negative ions

α - a lumped recombination coefficient

α_i - the electron-ion dissociative recombination coefficient

$N_e(z,o)$ - the initial electron density.

Two approximations are treated for the condition of weak ionization, which is defined by the condition $N_e(z,o) \ll 1/(\alpha t) \simeq 10^6 \alpha t$. In the daytime above about 70 km altitude, equation (2) reduces to

$$N_e\ (z,t) \simeq \frac{A}{D}\ N_e\ (z,o)\ e^{-2Dt} + N_e\ (z,o) \qquad (3)$$

In the nighttime below about 90 km, the equation reduces to

$$N_e\ (z,t) \simeq N_e\ (z,o)\ e^{-2At} + \frac{D}{A}\ N_e\ (z,o). \qquad (4)$$

It should be noted that in both cases, the decay rate of ionization is exponential and the initial decay rate is directly proportional to the initial ionization density. From the behavior of the ionization decay at early times, simple relationships between the initial phase excursion on an hf signal and the initial doppler frequency during the recombination process can be determined.

C. Maximum Values of Phase Change and Amplitude Change Caused by X-Ray Ionized Layers

Expressions for the peak value of phase path change and the absorption created by x-ray ionized layers can be developed by specialization of the previously discussed ionization formulas. All computations are based upon representation of the signal paths by equivalent vertical incidence paths, with equivalent vertical frequencies of reflection defined by $f_v = f_o \cos i$, where i is the angle of incidence of the ray path on the ionosphere and f_o is the transmitted frequency. The phase path effects are computed in terms of meters of phase path change and converted to fractions of a wavelength change in order to make them easily interpretable in terms of system characteristics of phase detection.

Two convenient formulas have been developed by Crain and Booker[3] to describe hf absorption phase path shift

$$\Delta A \simeq \frac{\sec i}{f_o^2} \frac{\Delta N_e \; T^3}{10} \text{ (db)} \qquad (5)$$

$$\Delta P \simeq \frac{\Delta N_e \sec i}{f_o^2} \text{ (meters)}, \qquad (6)$$

where T is the burst temperature measured in kev.

The maximum value of phase path change for a 1 MHz equivalent vertical frequency may be utilized as a parameter related to the detectability of a test with a given range-yield combination. Figure 12 illustrates the dependence of the smallest detectable x-ray yield vs. range for given values of the fractional phase path change parameter, ($\Delta P(\lambda) = \Delta P$(meters) (f_o/c). If detectability of a phase path change is related only to characteristics of a given hf detection system, then this graph can be utilized to directly determine the yield-range limit of the burst detection capability.

Absorption caused by transient x-ray ionization is a

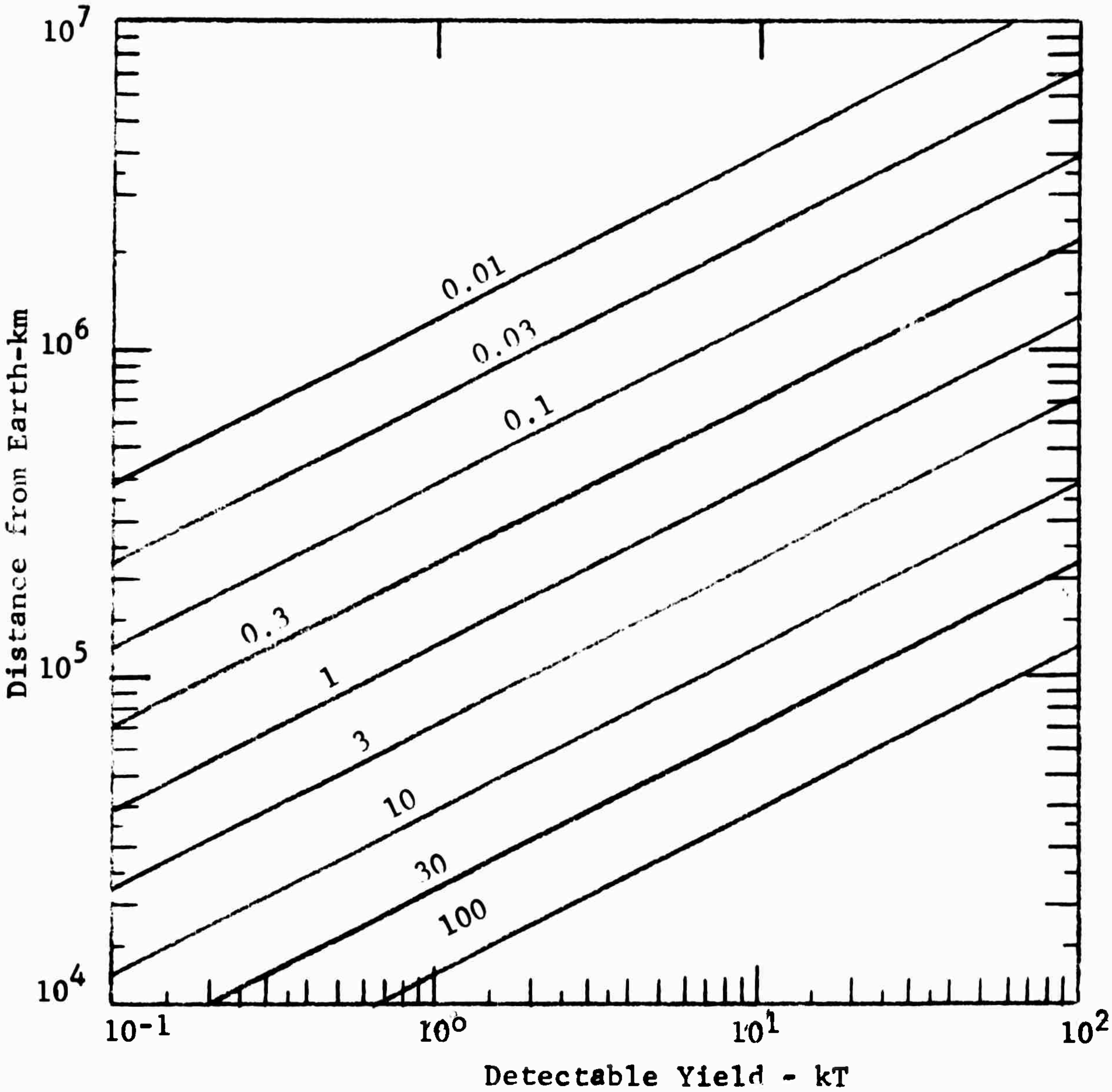

Figure 12 Detectable x-ray yield vs. range for parametric values of phase shift and peak electron density

somewhat less sensitive detection effect, as can be seen from comparison of equation 5 and 6. Because the ratio between absorption and phase path change for a given yield-distance combination is constant for a constant burst temperature, the fractional phase shift parameter of Figure 12 also can be utilized to determine the yield-range for a given value of absorption on 1 MHz.

The relationship between absorption and phase path change is

$$\Delta A = \Delta P \ (T^3/10) \ \ (f_o/c) \ (\text{db/wavelengths}) \qquad (7)$$

To convert the phase shift parameter to values for different frequencies the expression

$$\Delta P \ (f_v) = \Delta P \ (1 \text{ MHz})/f_v \ \ (\text{wavelengths}) \qquad (8)$$

must be used.

A potentially significant application of the parameter $\Delta P/\Delta A$ is the determination of burst x-ray radiation temperature. Figure 13 illustrates the temperature dependence of this ratio and in addition shows qualitatively the effect of potential errors in $\Delta P/\Delta A$ upon the derived burst temperature.

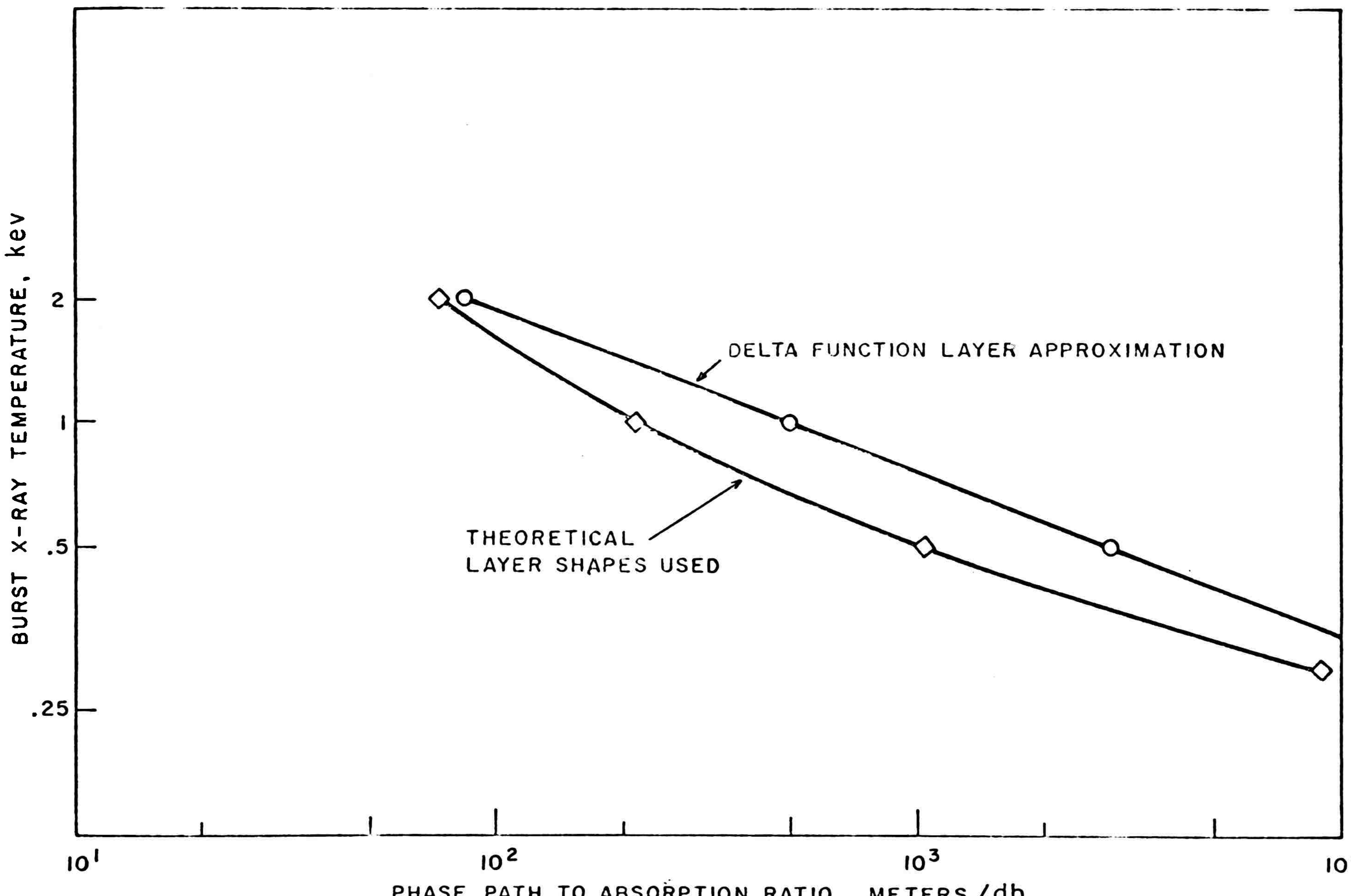

FIG. 13 BURST X-RAY TEMPERATURE VS. PHASE PATH TO ABSORPTION RATIO.

D. Rate of Change of Phase Path: Doppler Frequency

The transient phase shift produced by nuclear burst ionization is of positive sense, that is, the phase path is shortened. Consequently the doppler frequency induced on the hf signal over the interval of several milliseconds during development of the ionized layer is positive and of very large value. Because the time resolution and bandpass requirements would seem to preclude detection of the positive doppler transient, the discussion of this section will be limited to the negative doppler frequency induced by the decay of the ionized layer.

The doppler frequency is the time rate of change of the phase path,

$$f_d = - f_o \; (\Delta P/\Delta t) \; c. = \left(\frac{e^2}{c\, \epsilon_o m}\right) \frac{\sec\, i}{f_o} \; \frac{\Delta N_e}{\Delta t} \simeq 2.7 \times 10^{-4} \frac{T\,(km)}{f_v\,(MHz)} \frac{\Delta N_e}{\Delta t} \qquad (9)$$

The daytime and nighttime thin layer ionization decay formulas which were developed in section B have the same exponential decay form. The time dependence of the phase path decay and doppler frequency is expressed by

$$f_d = 5.4 \times 10^{-4} \; \frac{T \; AN(z_o, o)}{f_v} \; e^{-2At} \quad \text{for night} \qquad (10)$$

and by

$$f_d = 5.4 \times 10^{-4} \; \frac{T \; AN(z_o, o)}{f_v} \; e^{-2Dt} \quad \text{for daytime.} \qquad (11)$$

At t = 0,these formulas yields a direct relationship between initial value of doppler frequency and the phase shift caused by the transient layer $f_d(o) = A \Delta P(o)$. Substitution of the appropriate constants into the parametric graphs of Figure 12 thus allows an x-ray yield - range dependence to be determined for any particular value of peak doppler frequency which may be measured by a detection system.

The exponential decay of the doppler frequency during ionization decay for weakly ionized transient regions usually will predominate for time intervals lasting from a few seconds after the burst until the ionization has dropped to a level several times ambient. Of particular interest from the standpoint of discrimation of burst induced doppler signals is the time decay of signals having frequencies which are only slightly larger than those due to natural phenomena. During periods of ionospheric travelling wave disturbances, solar flares, or other natural activity, the exponential decay characteristic of the burst effect may be masked by the natural effects. Hence, the power spectrum of the natural doppler frequency fluctuations may be the limitation to discrimination of burst effects from natural effects. The characteristic decay time of x-ray ionization in the thin layer theory is dependent upon altitude and local time and burst temperature.

E. Instrumental Factors Influencing Burst Detection and Discrimination

A number of characteristics of high frequency phase detection instrumentation must be discussed with respect to the measurable signal quantities: phase, doppler frequency, and amplitude. Often instrumentation which is designed to provide a very precise measurement of one of the above quantities does not provide adequate measurement of the others. It is the purpose of the discussion in this section to qualitatively outline the general trade-off areas available to nuclear test detection instrumentation without discussion of specific systems.

There are two types of hf phase sounding experiments. The first is an oblique incidence bistatic sounder which may have one or more transmission frequencies and for which there may be several ray paths having one or more hops between transmitter and receiver. This type of instrumentation typically is operated as a cw system with a highly sensitive phase-tracking output. A variation on this type of instrument is the direct readout of the doppler frequency signal by real or delayed time spectral analysis of an intermediate frequency signal in the range of a few Hz. A short path version of the multi-frequency cw phase sounder which ensures single hop propagation has been utilized by the author to obtain the data for the present study, as well as for nuclear weapons effects[(4)] and solar eclipse ionospheric studies.[(5)]

The second basic form of the phase sounder is the monostatic pulsed sounder in which one or more frequencies are transmitted as pulses which are phase-locked to a standard precision oscillator and which are detected by a phase coherent detector. The monostatic radar approach allows evaluation of effects on a simple vertical incidence ionospheric propagation path and has the additional advantage of providing both phase height and group height data. Table III outlines some advantages and disadvantages of each system.

Since the phase is arbitrary to within $2N\pi$ radians during the growth of the x-ray transient ionization, it appears that the maximum doppler frequency in the ionization decay period is a quantity which can more easily be related to burst yield and distance than can the positive phase transient. For very distant or low yield events in which the phase shift is less than a few tens of cycles, very low initial doppler frequencies will result. For this reason, we consider both initial doppler frequency and the time behavior of doppler frequency compared with the natural ionospheric perturbations as measurable quantities, rather than phase shift alone.

Detection of small amplitude changes caused by nuclear burst ionization absorption depends to a great extent upon the characteristics of instrumentation and propagation path. As noted in Table III long paths which can propagate a number of rays will have complicated fading patterns which may degrade

TABLE III

SYSTEM TYPE	ADVANTAGES	DISADVANTAGES
Long path, cw, bistatic	Narrow cw bandpass gives high phase detection sensitivity and high signal sensitivity. Long path gives good sensitivity to lower ionospheric effects may be used over inaccessible region. Output may be either phase or doppler frequency.	Long path and multiple ray paths makes signal interpretation difficult. Multiple paths may give high fading. Usually narrow bandpass precludes measurement of doppler frequency greater than 10 Hz.
Short path, cw, bistatic	High phase detection and signal sensitivity. Short path gives better physical interpretation of signal effects in terms of ionospheric effects. Fewer signal paths makes fading effects less severe hence better interpretation of absorption.	Short path and high incidence angle makes system relatively less sensitive to D region effects.
Vertical incidence, monostatic, pulsed sounder	Highly interpretable data in terms of electron density profiles from both phase path and group path data.	Less sensitive to D region effects. Large bandpass to detect pulses may degrade sensitivity. Inter pulse phase coherence may be lost on rapidly varying phase signal. Smaller duty cycle requires longer integration time for equivalent phase sensitivity, poorer time resolution on fast events.

Additionally it should be noted that high phase sensitivity and wide band doppler readout are relatively incompatible in that phase trackers are inherently narrow band and hence usually would not admit signals with apparent doppler frequencies above a few tens of Hz. All phase tracking systems have the added problem that rapid phase changes such as occur in the positive phase path excursion in the x-ray ionization transient may induce an ambiguity of $N 2\pi$ in the phase record. This may be removed only by integration of the doppler frequency signal during the recovery phase.

the ability to discriminate natural from nuclear effects. It appears that on a short path, where fading is generally the result of interference between E and F region reflected rays or between two magnetoionic components, an absorption change of 3 db or greater would be detectible and interpretable as a nuclear effect. This statement is based upon the amplitude analyses carried out on the present project. Transient absorption levels between about 0.5 and 3 db during the nighttime would probably be interpretable as nuclear burst effects. During daytime, it is doubtful that either a transient absorption increase of less than 3 db or its decay in time would be detectible above the natural ionospheric variations, nor would they be interpretable as a nuclear effect. On this basis, the conclusion of Crain and Booker as to the relative insensitivity of amplitude changes as nuclear ionization detection quantities is reinforced.

F. Discrimination Between Nuclear Burst Doppler Frequency Peak and the Naturally Occurring Doppler Frequency Values

In this section we examine the distribution in doppler frequency experienced by a variety of hf phase path measurement systems and interpret these values in terms of the discrimination level above which a nuclear burst induced doppler frequency could be recognized.

The average diurnal variation in doppler frequency on three frequencies transmitted over a short path (800 km) as a function of local time is illustrated in Figure 14, a-c. Here, doppler frequency is computed on minute averaging intervals without respect to mode changes, changes of propagation path characteristics, etc. This type of output is what one would expect when comparing possible burst effect peak doppler frequency with normal background doppler frequency. A distribution of observed average negative doppler frequencies for each transmitted signal frequency is plotted in Figure 15. From this distribution one can determine the percentage of naturally occuring doppler frequency which is as great as or greater than that caused by any given level of burst yield and distance. The doppler frequency distributions at each frequency do not show measurable frequency dependence. This similarity of both the distribution and the magnitude of maximum doppler frequencies is partially peculiar to the short path experiment in that large value doppler disturbances over a single hop daytime path are rarely the result of either reflection height changes or changes in electron content along the path alone. Rather, the causes occur simultaneously and thus the frequency dependences (which are opposite) tend to cancel. The approximate equivalent vertical frequencies for the 4, 6 and 9 MHz signals are 2, 3 and 4.5 MHz respectively. It is clear from interpretation of this data base, that burst detection by

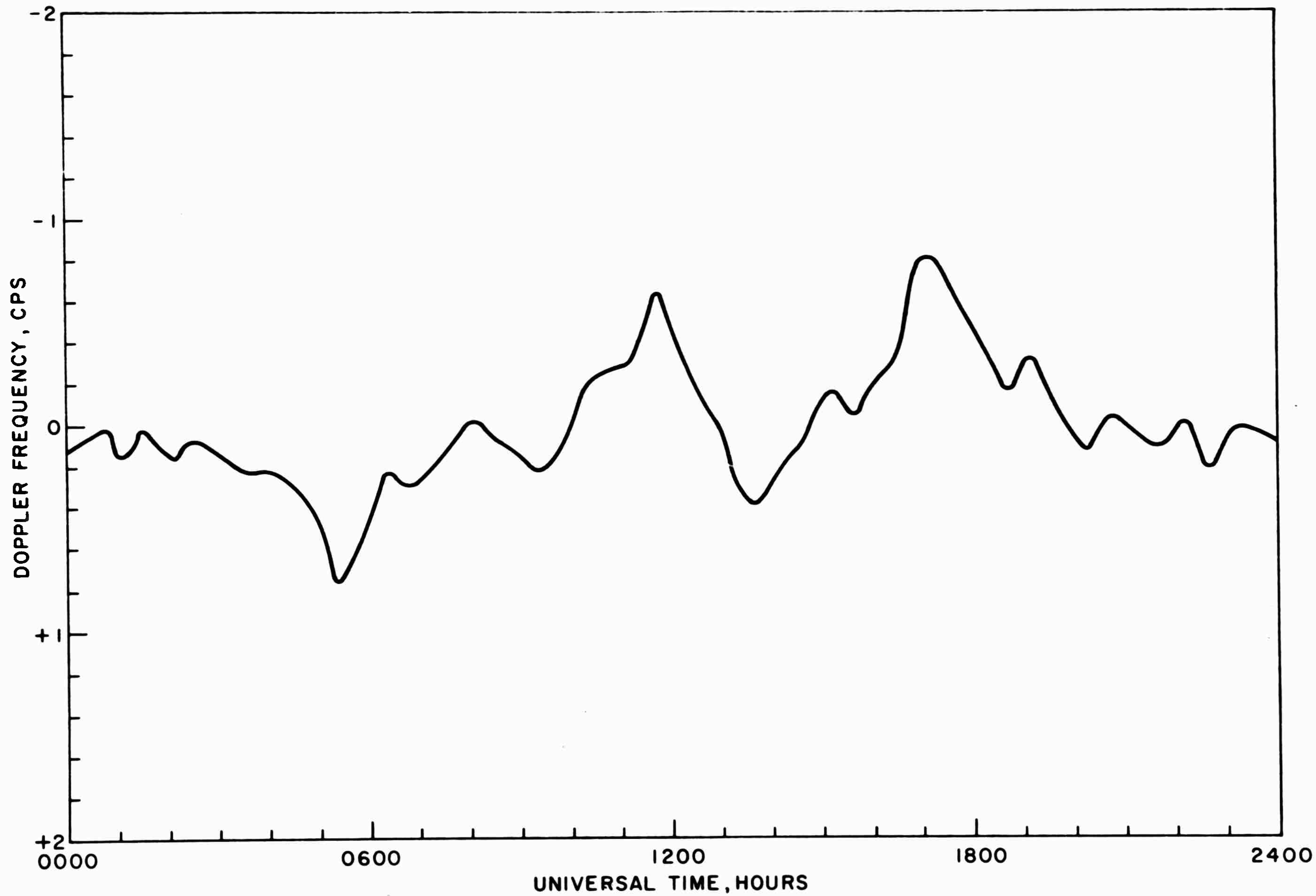

AVERAGE DOPPLER FREQUENCY vs. TIME
(25 DAY AVERAGE) 4 mc

Figure 14 a

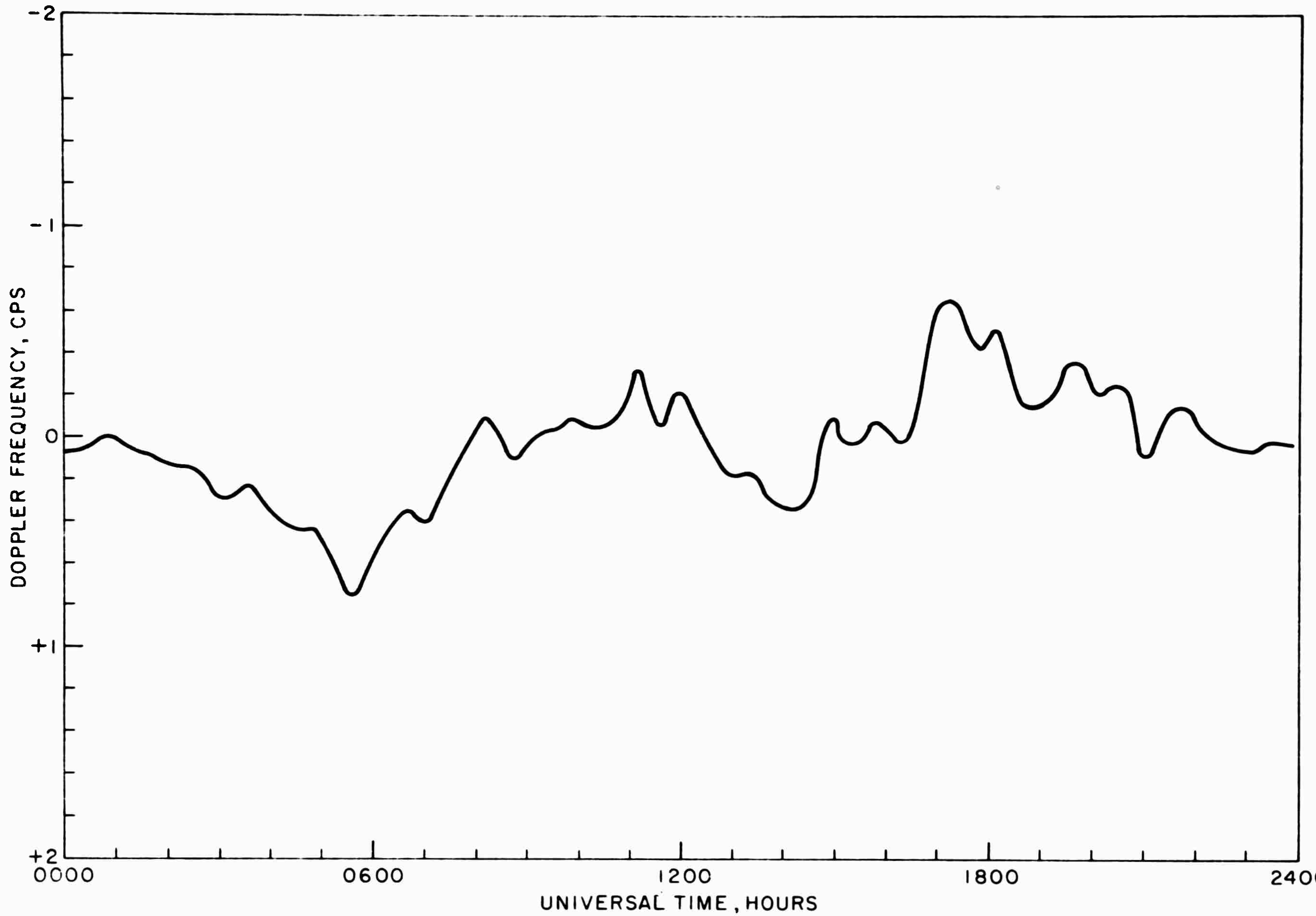

AVERAGE DOPPLER FREQUENCY vs. TIME
(25 DAY AVERAGE) 6mc

Figure 14 b

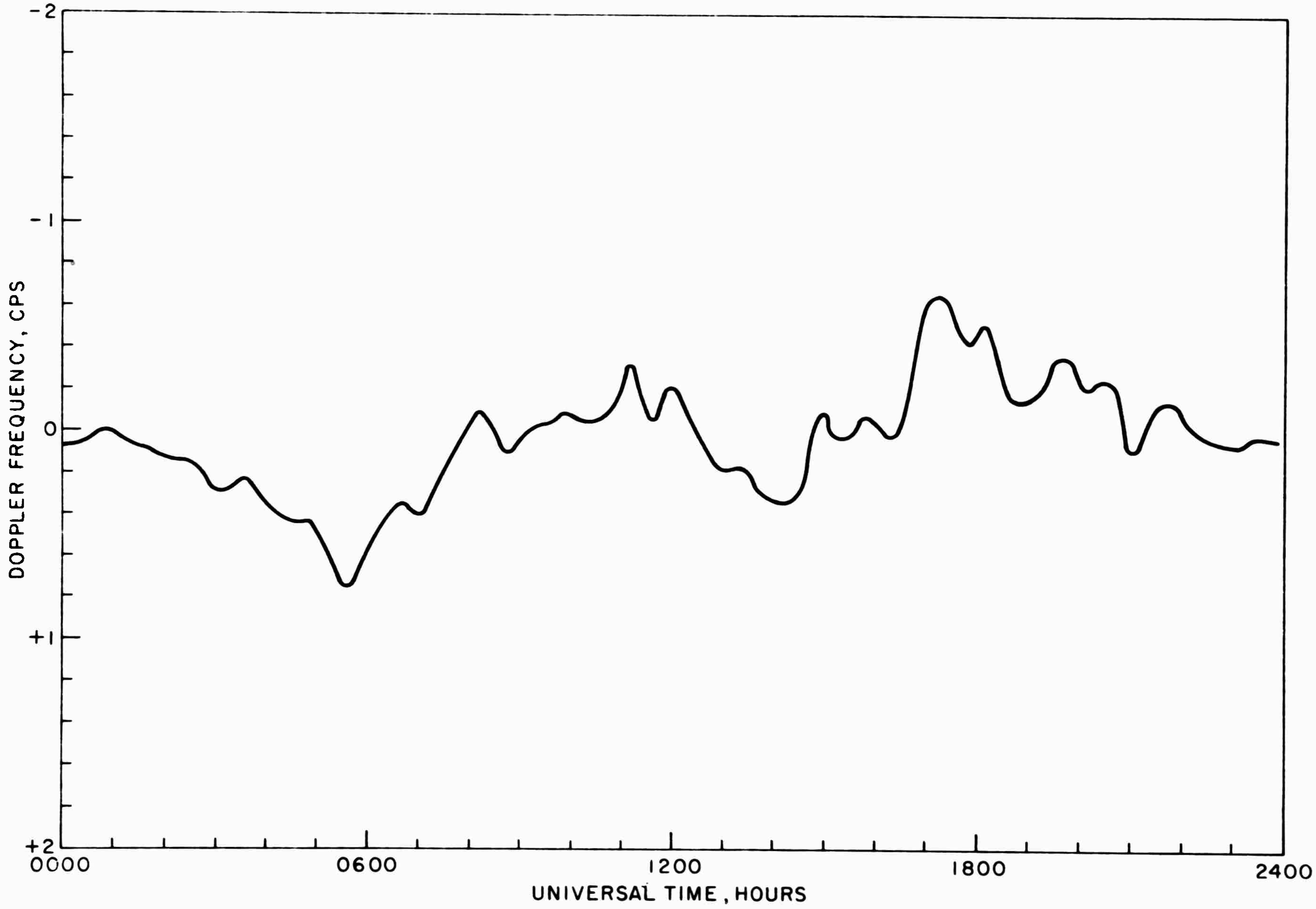

AVERAGE DOPPLER FREQUENCY vs. TIME
(25 DAY AVERAGE) 6mc

Figure 14 c

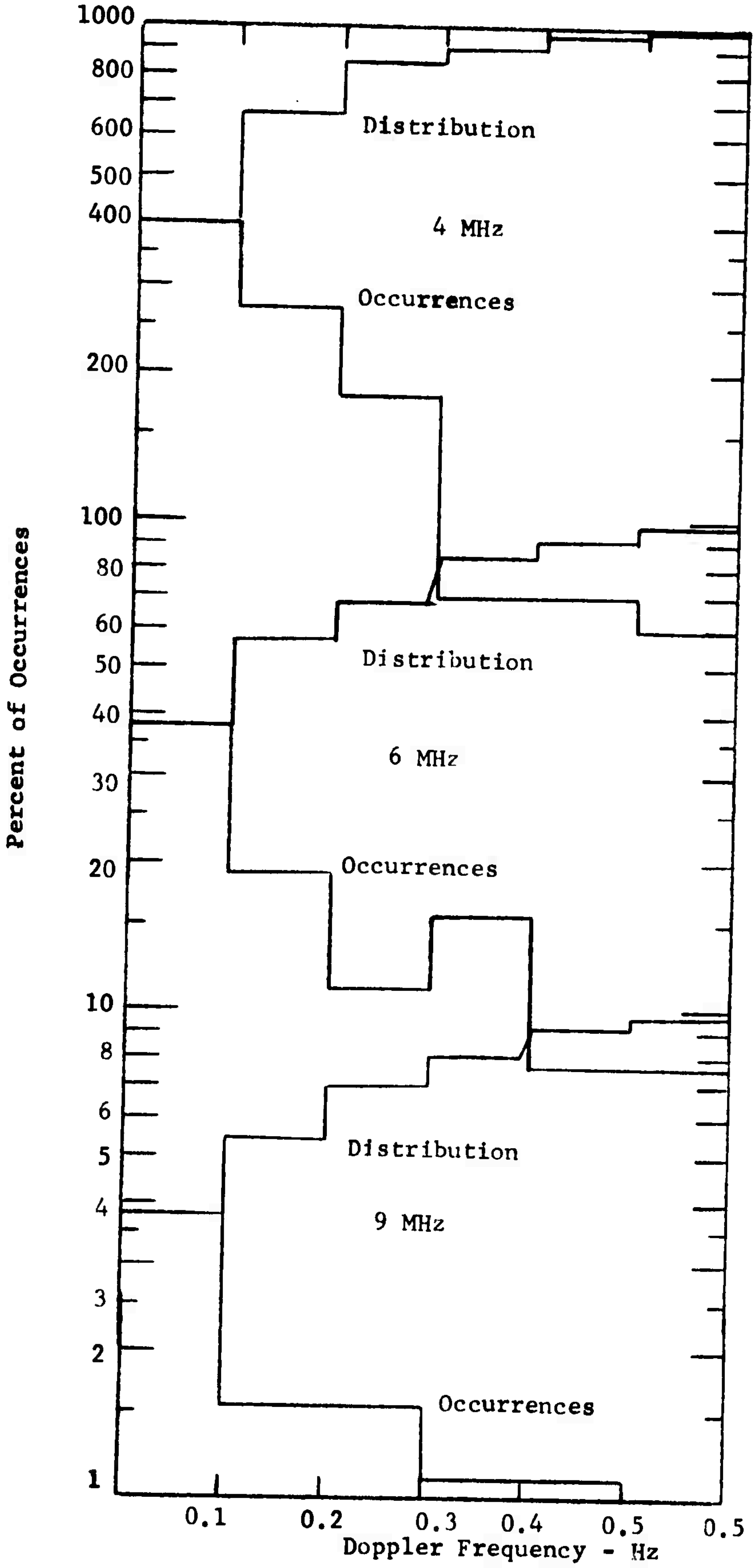

Figure 15 Distribution of average negative Doppler Frequency on 3 frequency HF experiments

doppler frequency measurement is most advantageous at the lower frequencies. In each case, the data show that 90 percent of natural ionospheric disturbances for this particular experimental time and location had a maximum negative doppler frequency excursion of 0.5 Hz or less. Positive doppler frequency excursions were not studied.

The distribution of natural doppler frequency excursions may be converted to an equivalent vertical frequency of 1 MHz. From this data base (at 4 MHz) we conclude that 90 percent of the naturally occurring doppler excursions for 1 MHz equivalent vertical incidence occur at values below about 0.2 Hz. This may be directly related to the parametric yield-range detection curves of Figure 12. We find from this process that 90 percent of the natural disturbances have an equivalent transient phase excursion of about 20 wavelengths; hence, bursts with yield-range parameters above this value have effects greater than 90 percent of the natural effects. For this example, a nominal radiation temperature of 1 kev was chosen. Examples may be devised for the other radiation temperatues, other propagation paths, or for other equivalent vertical frequencies. It should be noted, however, that the results presented in this example in terms of detection criteria are strictly valid only for the present short hop experiment in its low latitude location. Doppler frequency distributions for temperate latitudes may not be drastically different but the detailed circumstances of a given propagation experiment should be used to determine its nuclear burst detection sensitivity.

Of added importance to determination of the level at which natural and nuclear burst disturbances can be discriminated is the study of solar x-ray flare induced doppler frequency. Reference (6) provides a data base for this study. The distribution of negative doppler frequency occurrences vs. magnitude of the peak doppler frequency observed are plotted in Figure 16. As before, the percentage of occurrences of high negative doppler frequency is fairly small. We again take the level of doppler frequency below which 90% of natural solar flare decay doppler occurs. This frequency is about 0.4 Hz which corresponds to an initial phase path shift of 40 wavelengths. Because this data is not selected on the basis of an individual frequency or propagation system, it might be considered to be typical of the detection limits available to a variety of systems. More importantly, it shows that even though the positive or growing phase of a solar flare contributes ionization over the ambient level, the decay of this ionization is not rapid enough in the daytime to induce large values of maximum negative doppler frequency. This behavior is attributable to the nontransient nature of the x-ray flare as well as to the generally lower temperature or softer nature of flare x-ray emission as compared with nuclear burst radiations.

Study of the characteristic doppler frequency during layer formation and comparison with other sources of doppler frequency disturbance have been reported previously on this

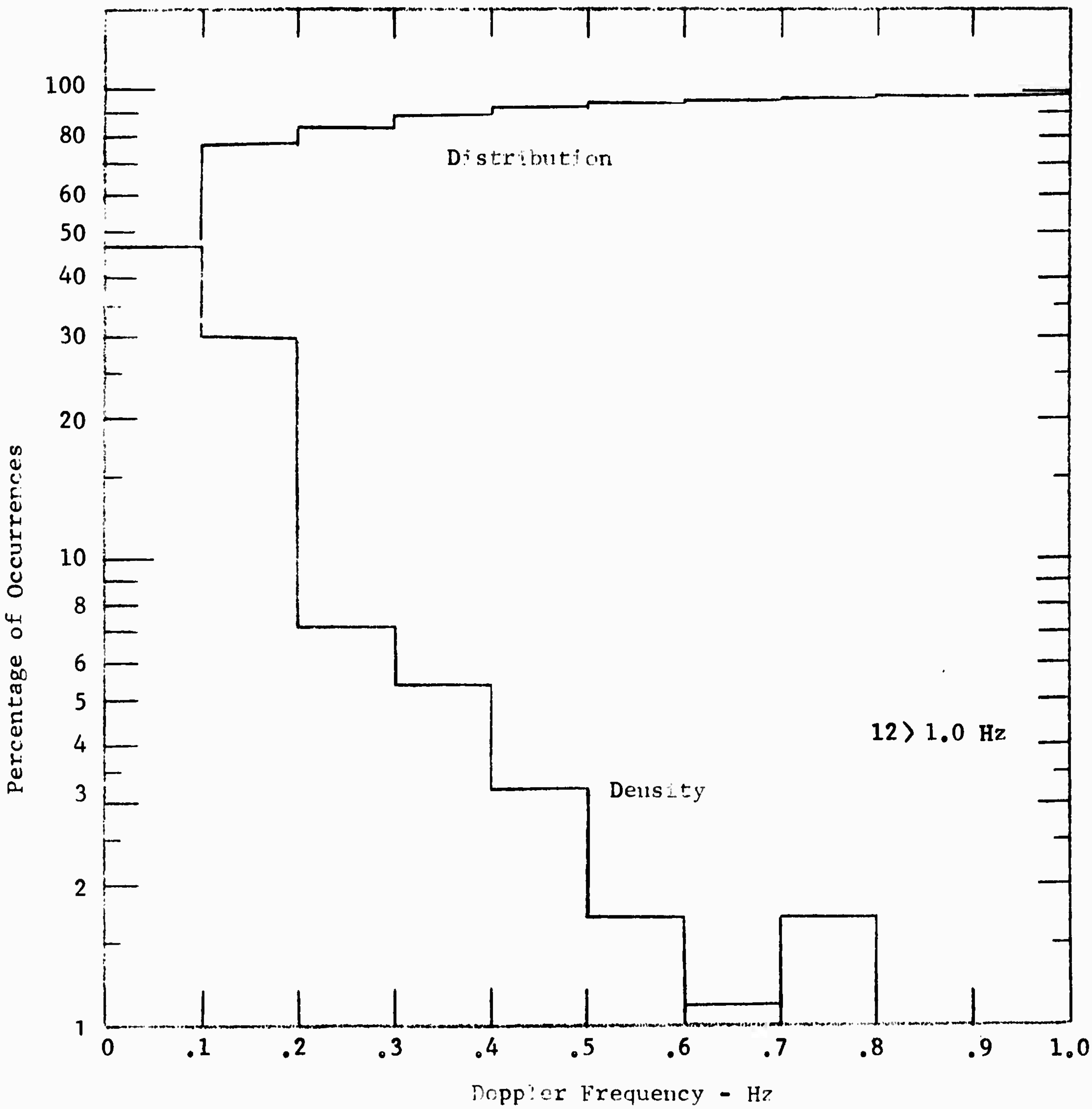

Figure 16 Plot of number and distribution of negative doppler frequency occurrences after solar flares.

contract.[1] In essence, one can summarize these results with respect to doppler frequency by their characteristic exponential doppler frequency variation in time during layer formation, and a much less well defined behavior during layer decay. During layer formation, the doppler frequency is of positive sense, hence would not be confused with the decay of nuclear ionization. During layer decay in the evening the doppler frequency is negative, but the data samples analysed to date do not indicate a consistent behavior except the generally quite low value of peak doppler frequency, less than 1 Hz.

Another source of doppler frequency disturbance which is mainly present at nighttime in the low latitude data examined on the present program is ionospheric motion and the presence of travelling ionospheric disturbances. These disturbances usually produce very large and long lasting periodic doppler disturbances. Times of passage of the larger disturbances are typically 10's of minutes with peak doppler frequencies as large as 1 to 2 Hz. The generally long term periodic changes in doppler frequency may serve to distinguish these natural occurrences from nuclear induced effects, but more effort on obtaining distribution of doppler frequency and period of such disturbances in higher latitudes would be valuable.

In order to determine whether nuclear burst ionization effects upon hf phase or doppler frequency can be detected at levels extending down into the ambient ionospheric "noise" level, the doppler frequency during selected dawn and daytime periods was subjected to harmonic analysis. This analysis and typical results are described in Section II and the results are applied to nuclear burst discrimination herein.

For purposes of comparison of the naturally induced doppler frequency fluctuations (whatever the cause) with small doppler frequency variations which would be produced by nuclear burst ionization decay, we analyse the thin layer nuclear burst ionization approximation in terms of the doppler fluctuation power which it would introduce to an hf signal.

Utilizing the expressions for the decay of negative doppler frequency at nighttime and at local daytime following a transient ionization event (equations 10 and 11) the doppler frequency autocovarience function is found to be

$$C_{fd} = \langle fd(t)\ fd(t+\tau)\rangle = K^2\ N_{eo}^{2}\ e^{-2Bt},$$

where $B = D \cong 0.3$ in the daytime case, and $B = A \cong 1 \times 10^{-2}$ for the nighttime case, for a 1 kev burst radiation temperature. The fluctuation spectral power density is found from the autocovariance function by

$$P(f) = \frac{1}{\pi} \int_0^\infty \cos\omega t \quad C_{fd}\ dt = \frac{K^2\ N_{eo}^2}{\pi} \quad \frac{B}{B^2 + \omega^2}\ .$$

In this case the fluctuation power density is frequency independent if the frequency of interest is less than the value of the reciprocal of the characteristic decay time, i.e. $\omega^2 \ll B^2$. We use this approximation to compare with the values of fluctuation power obtained in Section II, for the flat or "white" portions of the spectra. Substituting the values of the constants into this formula for power density and using the power and equivalent vertical frequency for the 4 MHz experimental result, we find that the peak value of electron density fluctuation in the daytime is N_e = 0.7 to 2.5 x $10^3 cm^{-3}$. The lower limit approximates geomagnetically quiet conditions and the upper limit is representative of moderately disturbed conditions. In terms of the parameters related to nuclear burst detection, this ambient electron density fluctuation level is equivalent to a range of maximum or transient initial phase path change of 2 to 7 wavelengths or a minimum burst x-ray yield of 1.3 kt at 10^5 kilometers. The equivalent value of initial doppler frequency which would be produced in the decay of such a layer is between 0.02 and 0.07 Hz. One may relate the discrimination level defined herein to cases of other levels of geomagnetic activity through use of Figure 10. One can easily see that the average fluctuation power increases rapidly with increasing geomagnetic activity, so that the geomagnetic activity index may serve to some extent as an index of the nuclear effects discrimination level. It is also clearly evident that at high levels of geomagnetic activity, the power to discriminate nuclear induced doppler frequency fluctuations from natural perturbations is degraded at least by an order of magnitude, i.e. by two orders of magnitude in the doppler frequency fluctuation power.

IV. CONCLUSIONS

This study has presented results showing the effects of natural ionospheric disturbances at low latitudes upon high frequency phase path and amplitude measurements. Analytical methods of determining the electron density profile changes in the lower ionosphere from phase path and amplitudes were developed and applied to the development of the ionospheric E region during a number of dawn intervals. The growth of the lower ionosphere during dawn introduces characteristic signatures on the high frequency doppler signal and on the amplitude fading pattern. During the daytime, the phase path is characterized by very low rates of change on the short single hop paths investigated, and consequently the doppler frequency induced upon the signal is very low.

Application of the knowledge of the average ionospheric electron density profile, its characteristic changes at dawn and in the daytime, and the effects induced upon hf phase and amplitude measurements is made to determine the level of nuclear burst ionization detection and the ability to discriminate nuclear ionization effects from natural effects. Analyses which yielded the best detection-discrimination criteria were: (1) comparison of peak excursion values of negative doppler frequency in the natural ionosphere due to natural perturbations with those expected from nuclear bursts; (2) comparison of the level of fluctuations of doppler frequency by the decay of nuclear burst ionization (in daytime) with the natural doppler frequency fluctuation level. In both cases examples of the ability to detect nuclear burst ionization and and discriminate between it and natural ionization effects are given for the high frequency path data which was analysed. The examples are strictly applicable to low latitudes, low to moderate levels of geomagnetic activity and to short single hop propagation paths.

The results presented herein suggest the following general conclusion: the level of detectible nuclear burst effects for a given high frequency detection system is usually well below the level at which natural ionospheric changes will introduce interference or will mask the nuclear effects. Although the ability to detect transient phase shifts caused by nuclear ionization produces a very sensitive burst detection parameter, the ambiguity created by more than one cycle shift for x-ray yield larger than about 0.7 kt at 10^5 km range precludes adequate determination of the yield distance relationship. Comparison of peak negative doppler frequency or doppler fluctuation power from nuclear effects with the natural levels has been shown to define a discrimination level above which nuclear effects can be identified. For the particular data sample analysed, these levels were about 10 to 30 kt x-ray yield and 1 to 2 kt x-ray yield respectively at 10^5 km range. Geomagnetic activity tends to degrade both of these discrimination levels, the latter by about an order of magnitude from geomagnetically quiet to geomagnetically disturbed condition ($\Sigma K_p \simeq 5$ to $\Sigma K_p \gtrsim 20$).

Finally, it was shown that the signature of the decay of nuclear burst ionization and the hf signal doppler frequency will be exponential in form over a short period of time and the time constant of decay will depend upon the burst x-ray radiating temperature and local time.

REFERENCES

1. Sears, R. D., "Analysis of Low Latitude D and E-Region Data", Semi-annual report number 3 on contract N 00014-66-0030. November 1967.
2. Bogush, R. L., "Approximate Series Solutions for the Three-Species Atmospheric Deionization Differential Equations," RM 65-TMP-7. February 1965.
3. Crain, C. M., and H. G. Booker, J. Geophys. Res. 68, 2159, 1963.
4. Sears, R. D., "Conjugate VLF and HF Measurements," in Symposium on Debris Motion and Ionospheric Effects, DASA Data Center Special Report 12, 1963.
5. Sears, R. D., "Effects of the November 12, 1966 Solar Eclipse on High Frequency Phase Path and Amplitude Measurements", paper presented at the 1966 Solar Eclipse Conference at Sao Jose dos Campos Brazil, February 1968.
6. Baker, D. M., N. Chang, K. Davies, R. F. Donnelley, and J. E. Jones, "A Review of Some Ionospheric Studies Based Upon HF Doppler Techniques", November 1967, ESSA Technical Report Number 387.

UNCLASSIFIED

Security Classification

DOCUMENT CONTROL DATA - R&D

(Security classification of title, body of abstract and indexing annotation must be entered when the overall report is classified)

1. ORIGINATING ACTIVITY (Corporate author)	2a. REPORT SECURITY CLASSIFICATION
IIT Research Institute	Unclassified
	2b. GROUP

3. REPORT TITLE

Analysis of Ionospheric Data

4. DESCRIPTIVE NOTES (Type of report and inclusive dates)

Fourth Semi-annual Technical Report - 1 Oct. 1967 to 31 March 1968.

5. AUTHOR(S) (Last name, first name, initial)

Sears, Robert D.

6. REPORT DATE	7a. TOTAL NO. OF PAGES	7b. NO. OF REFS
June 21, 1968	66	6

8a. CONTRACT OR GRANT NO.	9a. ORIGINATOR'S REPORT NUMBER(S)
N00014-66-C0030	
b. PROJECT NO. Office of Naval Research	V6061 (Formerly T6142)
c. ARPA Order #749	9b. OTHER REPORT NO(S) (Any other numbers that may be assigned this report)
d.	

10. AVAILABILITY/LIMITATION NOTICES

The distribution of this report is unlimited

11. SUPPLEMENTARY NOTES	12. SPONSORING MILITARY ACTIVITY
	ARPA

13. ABSTRACT

The average and short term fluctuations in apparent doppler frequency imposed upon three high frequency short-hop propagation paths are described. The average variation in doppler frequency during development of the reflecting region at dawn for both geomagnetically disturbed and quiet conditions can be characterized by an exponentially decaying positive doppler signal. The small scale doppler frequency fluctuations are analyzed by power spectral analysis techniques. It is shown that the power spectra usually have a constant spectral intensity at high frequencies (e.g. a white spectrum), and a slightly increasing spectral intensity at lower frequencies (e.g. a pink spectrum). The power contained in the white portion of the spectrum is shown to be correlated with the geomagnetic activity index ΣK_p.

The average changes in doppler frequency for quiet and disturbed daytime periods are related to the determination of the level of range and x-ray yield at which nuclear bursts in space may be detected against the natural background. Also, the natural fluctuation level of the hf doppler signals is related to the level of x-ray yield and range at which nuclear burst effects can be distinguished from the natural doppler "noise" level of an hf detection system.

DD FORM 1 JAN 64 1473

Security Classification